Wesleyan University Physics Department

Cooperative Dynamics in Supported Polymer Films

by

Paul Z. Hanakata

Class of 2014

A thesis submitted to the faculty of Wesleyan University
in partial fulfillment of the requirements for the
Degree of Bachelor of Arts
with Departmental Honors in Physics

Middletown, Connecticut April, 2014

Abstract

Ultra-thin polymer films have ubiquitous technological applications, ranging from electronic devices to artificial tissues. These nanoconfined polymer materials, typically with thickness less than 100nm, exhibit properties that are different from their bulk counterparts. Despite extensive efforts, a definitive picture of nanoconfinement effects on dynamics, such as the glass transition temperature and fragility (two of the most important properties for amorphous polymer processing) has yet to emerge. In particular, property changes in the dynamics of supported polymer films in comparison to bulk materials involve a complex convolution of effects such as boundary thermodynamic interactions, boundary roughness and compliance, in addition to finite size effects due to confinement. In this thesis, we consider molecular dynamics simulations of substrate-supported, coarse-grained polymer films where these parameters (e.g polymer-substrate interaction) are tuned separately to determine how these variables influence polymer film molecular dynamics. All these variables significantly influence the film dynamics, but all our observations can be understood in a unified framework through a quantification of how these constraining variables influence string-like collective motion within the film. This scale serves a measure of the scale of cooperatively rearranging regions, hypothesized in the Adams-Gibbs theory to describe molecular relaxation.

A challenge to this framework is that this cooperative dynamical scale is not readily accessed in experiments. Therefore, we investigate the relatively high mobility interfacial layers near the polymer-air interface, whose thickness ξ grows in a similar fashion to the scale of collective motion within the film. We find the precise scaling relation between ξ and the average length L of string-like

particle exchange displacements (strings). This is the first direct evidence that the thickness of the interfacial mobile layer is related to the scale of collective motion within the film. Moreover, this relation links ξ to relaxation time via the Adam-Gibbs relation, so that changes in ξ can be directly connected to the changes in film glass transition temperature. Our findings are consistent with other recent studies, theoretically predicting or providing indirect evidences regarding the relation of ξ to the scale of collective motion.

Acknowledgments

First and foremost, I would like to thank my advisor, Professor Francis Starr, for his guidance and support throughout the process of writing this thesis. Thank you for letting me join your lab in my freshman year, when I first fell in love with physics and the study of glass formation. Working as your research assistant has been the most valuable experience of my Wesleyan career. Without you, I will not be who I am today. It has been a pleasure and honor to work for you for almost four years.

Many thanks to Dr. Jack Douglas at the National Institute of Standard and Technology who has worked closely with me since my first project. His hard work and enthusiasm has always encouraged me to think and work outside the box. I will always be grateful to Dr. Fernando Vargas-Lara for introducing me to Professor Starr. Collaborating with my colleague Dr. Beatriz Pazmiño Betancourt has made my research career a lot more fruitful. To the current lab members, Josh, Hamed, Wengang, Neha, Wilson, and Wujie, thank you for always sharing your thoughts, jokes, and snacks. Special thanks to Yun Seong Nam for always being available to help. The physics department is where I made my home at Wesleyan and its faculty has given me invaluable lessons and support for which I am incredibly grateful.

I would also like to thank Wesleyan University for providing computational facilities and the ACS Petroleum Research Fund that support my research. This thesis would not have been possible without the financial support from Mr. and Mrs. Freeman throughout my four years at Wesleyan.

I cannot thank my family enough for the encouragement and prayers for my

pursuit in scientific work. Many thanks to Angela, who has been supportive and loving in any circumstances that I have been through. To my friends and housemates, thank you for sharing the ups and downs of these years.

Above all, I thank God, the Creator of this physical world full of mysteries for me to explore.

Contents

List of Figures

Chapter 1

Introduction

1.1 Polymers and a Brief Introduction to the Glass Transition

In 1959, Nobel Laureate physicist Richard Feynman in his famous lecture "There's Plenty of Room at the Bottom" proposed that properties of materials at nanoscale would present future technological applications [1]. His view on future technologies has brought attention of the scientific community to the explorations and manipulations of materials at nanoscale. A central goal of modern nanotechnology has been the realization of highly customizable structures, via either fine manipulation or self-assembly, that can have novel features when compared to bulk counterparts [2–4]. Polymers have played a substantial role in this development [5–7]. We encounter polymer-based products every day, primarily because polymer-based products are durable, light, and cost effective. The simplest case of a polymer is a linear homopolymer, a macromolecule that consists of the same type of N monomers forming a linear chain. Due to the complex nature of polymers, at low temperature, a bulk polymer is mechanically brittle like a solid,

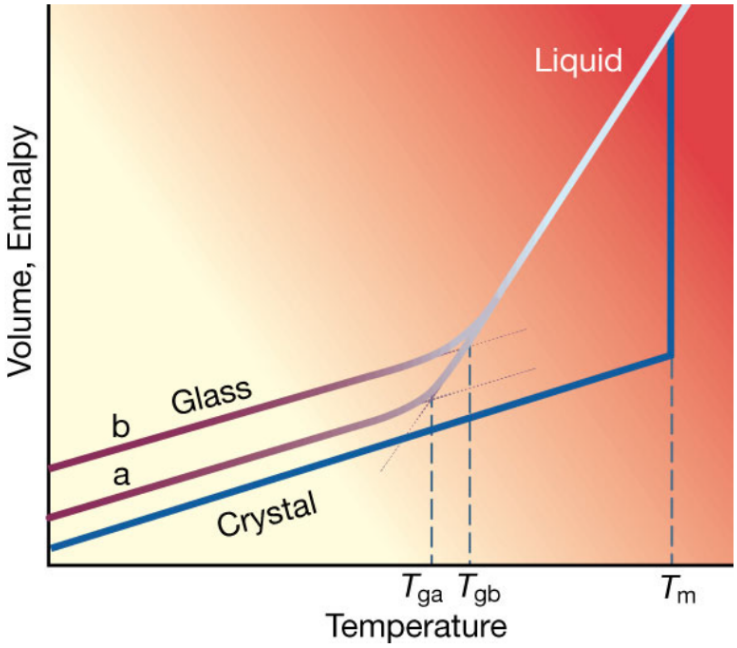

Figure 1.1: Volume or enthalpy of a liquid as a function of temperature at constant pressure. T_{m} is the melting temperature. A slow cooling rate produces a glass with glass transition temperature $T_{g\mathrm{a}}$. A fast cooling rate produces a glass with $T_{g\mathrm{b}} > T_{g\mathrm{a}}$. The figure is taken from Ref. [8].

but not necessarily in a crystalline state. Rather, polymers typically exhibit an amorphous structure in their solid state, referred to as the glassy state. Upon cooling, relaxation time or viscosity increases dramatically, and below a temperature, the so called glass transition temperature T_g, the timescale of the relaxation becomes greater than the experimental timescale. At this temperature, T_g, the polymer melt becomes a 'frozen liquid'. Naturally the location of T_g and changes in this quantity due to confinement are of great practical interest, since polymer processing relies on working with a fluid state.

Broadly speaking, the glass transition is a dynamic transition with no discontinuous changes in thermodynamics. Given that glass transition is a dynamic

phase transition, the observed T_g is dependent on the rate of cooling. In particular, the glass transition temperature is usually obtained by examining changes in slopes of thermodynamic quantities such as volume or enthalpy. Figure 1.1 is a schematic for how a fluid turns to a glass at different T_g when cooled with a different cooling rate.

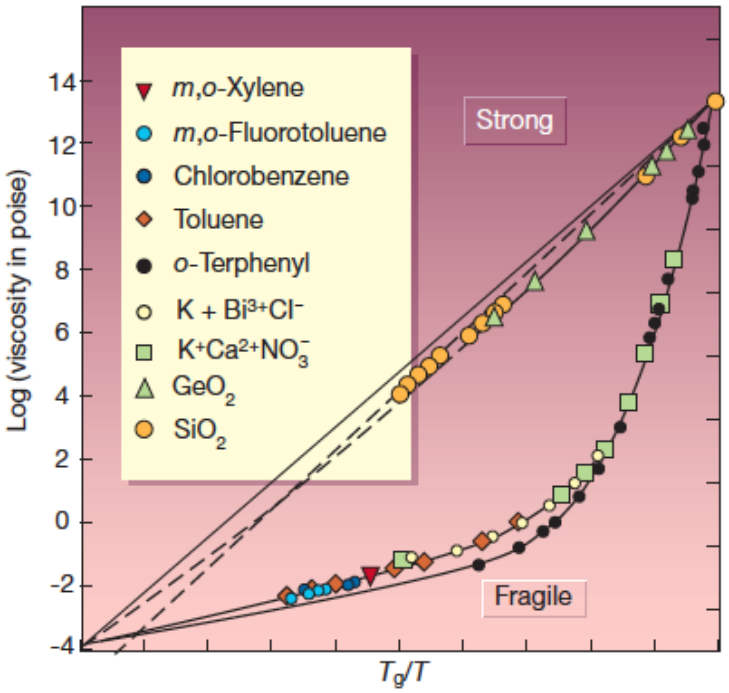

Figure 1.2: Viscosity of various liquid as function of T/T_g, known as Angell's plot. Strong glass formers exhibit Arrhenius behavior, whereas at low temperature fragile glass formers exhibit super-Arrhenius behavior, implying the temperature-dependence of the activation free energy ΔG in equation (1.1). Figure is taken from Ref. [8].

From kinetic measurements, increases in viscosity or relaxation time with decreasing temperature are observed in many glass formers. Figure. 1.2 shows that some glass formers like silica and germanium oxide exhibit an Arrhenius behavior

described by,

$$\eta = \eta_0 \exp\left[\frac{\Delta G}{k_{\mathrm{B}} T}\right], \tag{1.1}$$

where k_{B} is Boltzmann constant and ΔG is activation free energy. Materials following Arrhenius behavior are known as 'strong' glass formers. Other glass formers known as 'fragile' glass-formers exhibit non-Arrhenius behavior: logarithm of viscosity η does not scale linearly with $1/T$, as shown in figure 1.2. In a lab setting, T_g is often defined in practice as the T at which the relaxation time reaches 100s or viscosity reaches 10^{12}Pa·s [9]. Clearly, scaling T with T_g does not result in a simple collapsed curve (illustrated by figure 1.2). Hence, it is also important to understand the rate of change of viscosity (or relaxation time) at T_g, known as the fragility index m, which is commonly defined as

$$m(T_g) = \left.\frac{\partial \ln \eta}{\partial (T/T_g)}\right|_{T_g}. \tag{1.2}$$

Despite the significant changes in dynamics in the process of glass formation, there is little change in the amorphous structure of the melt. This raises many questions about the origins of glass formation. Understanding this non-intuitive phenomenon and constructing theories in an attempt to explain the changes in dynamics have been major research topics in glass-formation studies [8, 10, 11]. From technological applications, much effort has been put on tuning T_g of polymeric materials. For instance, occasionally it is desirable for some polymer-based products to remain in a liquid-like or mechanically brittle state at room temperature. Regarding this particular application, many studies are centered in T_g measurements [6, 7, 12].

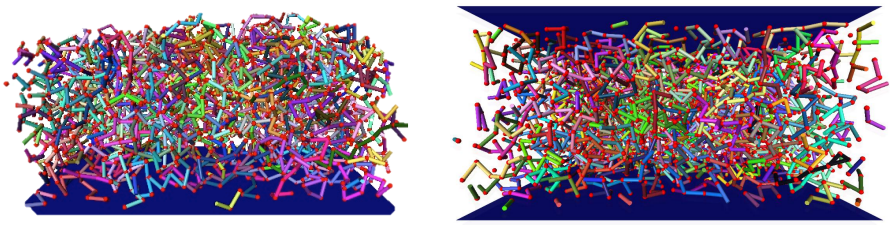

Figure 1.3: Schematic illustration of (a) a polymer film supported on a supporting substrate (supported film) and (b) a polymer film confined between two walls ("sandwiched" film).

1.2 Polymer Films

There have been great interest to utilize polymeric materials not only in a bulk form (large scale) but also in highly confined and nanoscale environments. In particular, ultra-thin polymer films have ubiquitous technological applications, ranging from electronic devices to artificial tissues [5, 7, 13, 14]. Commonly, there are three types of polymer films (illustrated in figure 1.3):

- Supported films are polymers that are supported on an attractive substrate.
- "Sandwiched" films are polymers that are confined between two walls.
- Free-standing films are polymer films with no confining wall (two free-interfaces). These films are obviously unstable above T_g.

There has been extensive experimental [15–23] and computational [24–29] studies of polymer films aiming for understanding the large property changes that are frequently observed under nanoconfinement, typically in a scale of $\lesssim$ 100nm, in relation to bulk materials. Changes in mechanical properties and the dynamical properties of amorphous polymer films bear particular importance when it comes to applications, and much of the effort in characterizing thin polymer films has centered on the measurements related to the stiffness of the films [30, 31] and the changes of molecular mobility as quantified by the glass-transition temperature

T_g [20, 32].

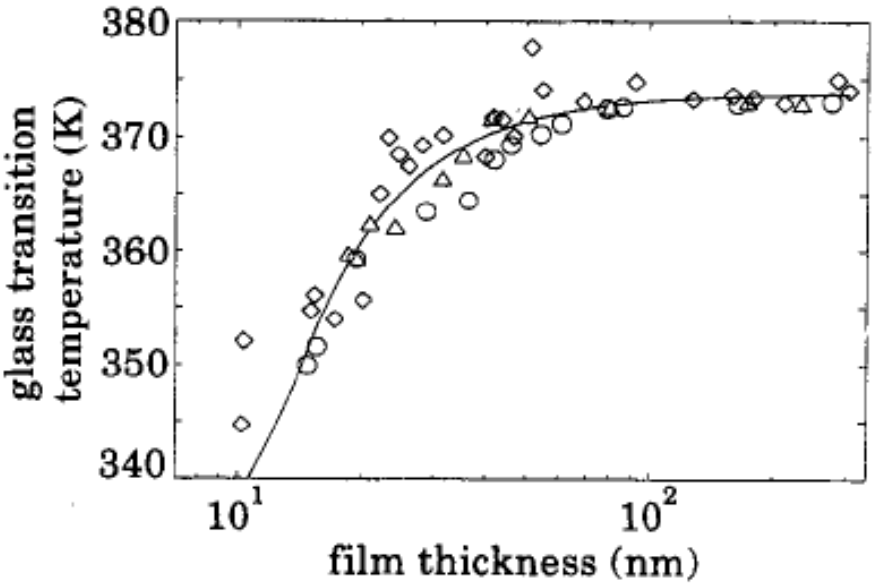

Figure 1.4: Depression of T_g in polymer films. T_g decreases with decreasing film thickness. This figure is taken from Ref. [15].

In the early 1990s, one of the first experimental observations of T_g shifts in polymer films relative to the bulk was reported by Keddie et al. [15]. Keddie et. al found that T_g of polymer films decreases with decreasing film thickness (see figure 1.4), and they suggested that the depressions of T_g are consequences of a liquid-like layer at the free surface. Many similar studies have confirmed that a free surface as well as a repulsive or neutral wall leads to enhanced dynamics and a reduction of T_g [16, 28, 33, 34]. In contrast, an attractive substrate, which typically slows down the dynamics near the substrate, results an increase in T_g [16, 18–22, 24, 26, 29, 35–37]. However, an attractive smooth surface with a relatively weak interaction may also enhance the rate of relaxation time and diffusion [17, 19, 22, 24, 38, 39], demonstrating that the polymer-substrate interfacial strength can

have significant effects on the polymer film dynamics. In particular, it has been noted that the enhancement or slowing of relaxation in supported films induced by two interfaces with different properties can complicate the interpretation of the thickness dependence of T_g [16, 19, 28, 29, 33, 35–37, 39]. The most prevalent type of polymer films are films supported on a solid substrate, where dynamics are often reduced near the substrate, but enhanced at the free surface. Various probe methods have been used to infer the variability of the mobility within the film by reporting T_g near the surface [15–17, 19, 33, 40], or reporting T_g as a function of distance z from the film boundaries [22]. Many phenomenological trends are clear from this wealth of data, but the understanding of the changes in the glass transition with confinement remains qualitative.

A popular picture to rationalize the changes of the film dynamics is a superposition of polymer layers different dynamics. In this perspective, any changes in the overall dynamics should be manifested locally, thus the interfacial layers are correspondingly expected to give the primary contribution to the observed changes in the overall dynamics. This layer picture of dynamics is often conceptually linked to the local changes in structure and free volume. In particular, free volume layer (FVL) ideas have been very influential in this thinking [20, 41, 42]. Near an attractive substrate, polymers are bound to the wall and density is increased (free volume reduced), leading to slower dynamics, while at the free surface of a supported or free-standing film (increased free volume), polymers have a relatively higher mobility. At the film center, far from both interfaces, the local properties are expected to be bulk-like.

Many experimental [15–23, 43], as well as computational [24–29] studies, have reported large property changes in thin films and have attributed these changes mainly to a convolution of interfacial thermodynamic interaction and geometrical confinement. There is also a growing awareness of the relevance of surface rough-

ness and boundary stiffness, as well as non-equilibrium residual stress effects in cast films [43–45]. Experiments on multi-layered films have shown that the effects of the free surface can be largely eliminated by placing films between stacks of nano-layered polymer with different species [46], suggesting that there is a scale associated with these dynamical changes. This leads to the question of whether the dynamics depend simply on the interfacial interaction, or are there other physically relevant characteristics of the interface that must be considered. After all, glass formation is a dynamical phenomenon so variables other than thermodynamic quantities –such as surface rigidity– might be relevant. This motivates an exploration of the effects of surface rigidity on properties of thin polymer films, a property that can be tuned in polymeric materials through cross-linking or via the control of the molecular structure [43–45].

It is a difficult matter to separate all of these different effects in experiments, and this thesis addresses this general problem through molecular dynamics simulations of substrate-supported, coarse-grained polymer melt films of variable thickness, where the polymer-substrate interaction is varied, along with the boundary roughness and rigidity. Since we can tune these parameters independently in simulation, we can obtain clear indications of how each of these variables influences the film molecular dynamics. After an analysis of how these diverse factors affect basic dynamic properties of the polymer film, we show that the dynamical changes under all these conditions can be organized and understood in a general way from how these constraining variables influence collective motion on the film.

1.3 Framework to Describe Film Dynamics

Given the sensitivity of the dynamics to the large collection of surface properties, a general question arises: how do we obtain a unified understanding of all these

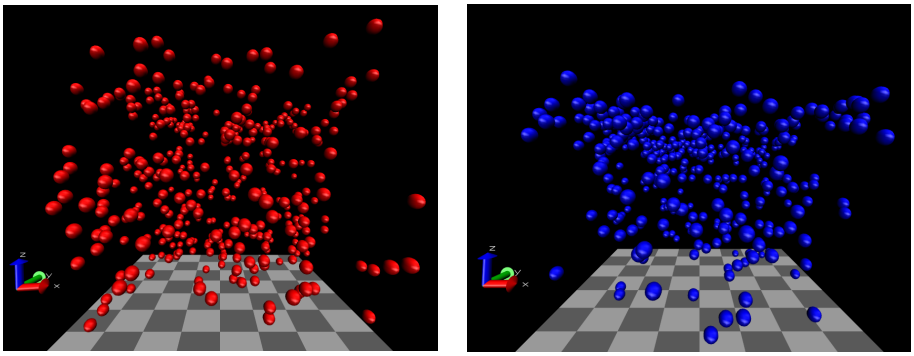

Figure 1.5: Simulation snapshot of most mobile particles in a supported polymer film at constant pressure $P = 0$ at (a) high temperature $T = 1.0$ and (b) low temperature $T = 0.5$. The most mobile particles tend to clusters at low temperature.

effects on the polymer dynamics? To answer this, we first need to understand the dynamics of glass formers at low temperature. In section 1.1, we briefly discussed how relaxation time or viscosity η changes dramatically with decreasing temperature. In particular, figure 1.2 illustrates how fragile glass formers exhibit non-Arrhenius behavior below an onset temperature T_{A} (often called the Arrhenius temperature): logarithm of viscosity η scales linearly with $1/T$ for $T > T_{\mathrm{A}}$ but then scales faster for $T < T_{\mathrm{A}}$. This indicates temperature-dependence of the activation free energy $\Delta G(T)$, which is commonly obtained from equation (1.1),

$$\Delta G(T) = k_{\mathrm{B}} T \ln \frac{\eta(T)}{\eta_0}. \tag{1.3}$$

In contrast, for a simple liquid, ΔG remains constant with respect to the changes in temperature. The activation energy of a simple liquid can be thought of as the amount of energy required for a system to rearrange into another state. To explain the non-Arrhenius behavior in fragile glass formers, Adam-Gibbs (AG) argued that the particles do not relax independently, but rather as a group of particles, recognizing that particles must move cooperatively at lower temperatures

in a regime where particles displacement become highly correlated [47]. A simple illustration of this scenario would be to take a look at the case where cars need to move cooperatively in a traffic jam. In this perspective, the slowing mechanism is associated with an increase in cooperativity. In particular, AG argued that the activation Gibbs free energy is extensive in the size of cooperatively rearranging regions (CRR). However, AG theory does not provide molecular definition of these CRR.

Adam-Gibbs [47] and the closely related random first-order transition (RFOT) [48] theories proposed that the variation of relaxation approaching T_g revolves around changes in an intrinsic scale. Glass-forming liquids generally exhibit dynamical heterogeneity, typically manifested by spatial correlations of mobility. In particular, those monomers with the greatest mobility tend to cluster [illustrated in figure 1.5], and subsets within these clusters move collectively in a string like-fashion, observed both in computer simulations [27, 47, 49–55] and colloidal experiments [56–59]. Simulations have identified cooperative rearrangement motions directly in bulk polymer materials that are linked to the structural relaxation time, and a similar connection has also been established inpolymer nanocomposites model [55, 60, 61]. These works argue that this intrinsic scale can be related to the characteristic scale of the string-like cooperative motion, providing a molecular realization of the abstract cooperatively rearranging regions invoked by AG and RFOT. This also suggests that ΔG grows in proportion to the scale of string-like cooperative motion. Accordingly, we aim to test the applicability of this scheme for dynamics of polymer films and further to test whether this approach can be applied universally to all films that have high variability in dynamics.

While using the string size as a way to charecterize CRR seems to be a promising way to generalize film dynamics, direct experimental observations of this string-like cooperative motion in molecular glass-forming liquids remains as a

great challenge. Therefore, we further aim to quantify a scale that can be directly measured in experiments and can potentially be linked to the scale of strings-like cooperative motion.

Several recent studies, both in computer simulations [26–29, 39] and experiments [22, 46], have shown that films are spatially heterogenous due to interfacial effects. By examining the dynamics locally as a function of distance z from the substrate or the free surface, one can find a quantifiable scale for the perturbation of interfacial dynamics [34, 39]. At this point it is natural to ask to what degree this scale relates to the scale of CRR. Stephenson and Wolynes [62] have argued, based on the RFOT theory and scaling arguments, that the interfacial mobility length of films should scale inversely to the configurational entropy of the films. This result, combined with results showing that the string length scales inversely to the configurational entropy [55], suggests that the interfacial mobility length should scale proportionally to the string length, and thus describes the temperature dependence of relaxation. Very recently, Simmons and coworkers [63] found that the interfacial mobility scale grows in proportion to the apparent activation energy for relaxation from molecular dynamics simulations of polymer films, suggesting that this scale provides an estimate of the collective motion scale in the AG model. These recent observations along with arguments by Stephenson and Wolynes [62] motivate us to find a precise functional form relating the size of strings-like cooperative motions and the interfacial mobility scale and to test whether using interfacial mobility scales in terms of AG theory can be universally applied to describe all film dynamics.

1.4 Contribution of This Thesis

Here we summarize our main findings reported in this thesis. Broadly speaking, we first characterize how interfacial properties alter dynamics, and then demonstrate how these changes can be rationalized from changes in molecular scale cooperativity. Finally, we show how this scale can be indirectly probed via changing the scale of interfacial dynamics. Below, we provide more detail:

- First, we investigate the dependence of the dynamics on two relevant variables, surface roughness and the polymer-wall interaction strength. Contrasting the effects of both rough and smooth walls on the local properties, we observe noticeable changes in the dynamics, characterized by changes in the film T_g and fragility, while only small changes are observed in static properties, such as density. We find that free volume ideas are not generally useful in predicting dynamics at the local level. We show that the surface thermodynamic interaction, substrate roughness and stiffness can all greatly influence the mobility gradient transverse to the substrate. Our general findings for changes in structure, dynamics, and the variation of T_g with surface roughness and interaction strength are consistent with earlier works [18, 22, 24, 28, 64, 65], but our findings considering fragility and regarding substrate stiffness are new.
- We characterize the dynamical changes in terms of a cooperative motion within the film, and in this way, we obtain a quantitative understanding on the wide variations in the temperature-dependence of the structural relaxation time with respect to the film boundary conditions and thickness. We test this predictive scheme for polymer films, where the inherent inhomogeneity of the dynamics of these materials makes it unclear whether the model should still apply. Encouragingly, we find that the scale of strings-like

cooperative motion in polymer films can be used to determine relaxation of polymer film in terms of AG theory and obtain a remarkable reduction of all our simulation data for structural relaxation time in thin polymer films based on this unifying framework. Further, we investigate the influences of confinement on activation free energy parameters.

- Lastly, we address how the scales of interfacial mobility of polymer films supported on rough or smooth surfaces with variable substrate interaction strength can be related to the scale of collective motion in films. Indeed, we find that the scale of string-like cooperative motion is proportional to the scale of the mobility gradient at the polymer-air interface to a good approximation. This offers a possible route to experimentally probe the scale of cooperative relaxation. At last, we use the interfacial mobility scales as substitutes of string size to determine relaxation time in terms of AG theory. We find a precise functional form relating the interfacial mobility scale to relaxation time. We provide a new unified theoretical framework to quantify relaxation time from interfacial scales. We also demonstrate that this functional form is universal for films with a wide range of dynamics. Our results are vital to experiments that try to extract relaxation time, as we provide the way to relate relaxation time to the interfacial mobility scale, which is experimentally accessible. With these findings, we are able to explore and further study other fundamental problems in glass formation.

Chapter 2

Modeling

Our findings are based on equilibrium molecular dynamics simulations of a common coarse-grained representation of polymer chains supported on a substrate with variable surface roughness and interaction strength. Specifically, we consider (i) a perfectly smooth substrate and (ii) an atomistically rough surface, where the roughness is controlled by the lattice binding strength. Non-bonded monomers and rough wall atoms interact with each other via a Lennard-Jones (LJ) potential, where a "force-shifted" truncation is used at $r_{\rm c} = 2.5\sigma_{ij}$ [66] (with σ being the monomer diameter),

$$V_{\rm sf}(r) = V_{\rm LJ}(r) - V_{\rm LJ}(r_{\rm c}) - (r - r_{\rm c})\frac{dV_{\rm LJ}(r)}{dr}\bigg|_{r=r_{\rm c}}, \tag{2.1}$$

where the LJ potential is defined as,

$$V_{\rm LJ}(r) = 4\epsilon\bigg[(\sigma_{\rm ij}/r_{\rm ij})^{12} - (\sigma_{\rm ij}/r_{\rm ij})^{6}\bigg]. \tag{2.2}$$

The index pair ij distinguishes monomer-monomer (mm), wall-monomer (wm), and wall-wall (ww) interactions. The LJ interaction is not included for the nearest bonded neighbors along the chain. Bonded monomers are connected by a harmonic

spring potential

$$U_{\text{bond}} = (k_{\text{chain}}/2)\big(r - r_0\big)^2 \tag{2.3}$$

with bond length $r_0 = 0.9\sigma_{\text{mm}}$ to avoid crystallization (equilibrium distance) and a spring constant $k_{\text{chain}} = (1111)\epsilon_{\text{mm}}/\sigma_{\text{mm}}^2$ [38]. We use this harmonic bond potential, rather than the often used finite extensible nonlinear elastic (FENE) bond potential [67], due to crystallization that we find using the FENE potential for films on rough surfaces. Ref. [68] has considered a more detailed study of this phenomenon.

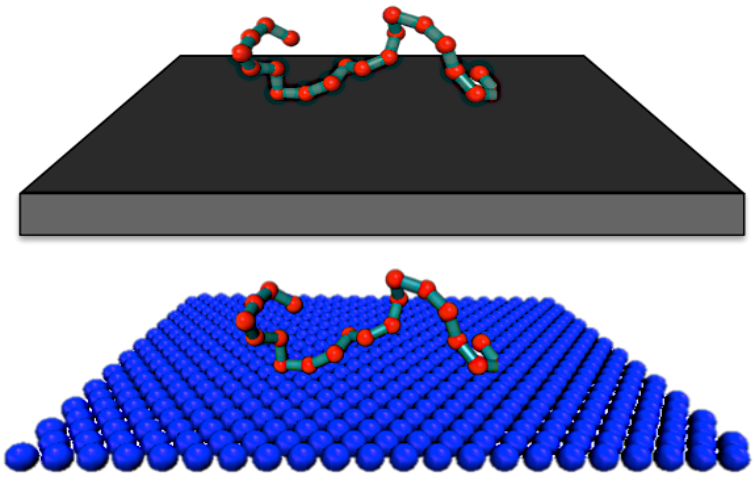

Figure 2.1: Schematic illustration of a polymer chain model supported on a smooth (top) or a rough surface (bottom). Size of the monomers and the molecular wall atoms are not drawn to scale.

For the perfectly smooth substrate, the interaction between a monomer and the substrate is given by a "9-3" LJ potential,

$$V_{\text{smooth}} = \frac{2\pi}{3}\epsilon_{\text{wm}}\rho_{\text{wall}}\sigma_{\text{ww}}^3\left[\frac{2}{15}\left(\frac{\sigma_{\text{wm}}}{z}\right)^9 - \left(\frac{\sigma_{\text{wm}}}{z}\right)^3\right], \tag{2.4}$$

where z is the distance of a monomer from the wall and ρ_{wall} is the number density of wall sites. This is the same model that we studied in our previous work [39].

To model the rough wall, we tether the wall atoms to the sites of triangular lattice [(111) face of an FCC lattice] with a harmonic potential $U_{\rm wall}(r_i) = (k_{\rm wall}/2)|\vec{r}_i - \vec{r}_{i\rm eq}|^2$, where $r_{\rm eq}$ denotes the equilibrium position of the triangular lattice and $k_{\rm wall}$ is the harmonic spring constant [26]. We choose the equilibrium distance between nearest neighbors to be $2^{1/6}\sigma_{\rm ww}$, where $\sigma_{\rm ww} = 0.80\sigma_{\rm mm}$ (which also sets $\rho_{\rm wall}$ for the smooth surface). We use various substrate interaction strengths $\epsilon_{\rm wm}$ between the rough surface and polymers, ranging from 0.4 to 1.0 $\epsilon_{\rm mm}$ (with a fixed $k = 100$); we vary the roughness of the wall by changing the strength of the wall rigidity from 10 to 100 (with a fixed $\epsilon_{\rm wm} = 1$).

To study the dynamical changes in polymer films, we simulate systems with a number of chains $N_{\rm c} = 200$, 300, 400, 600, 1000, or 1200 of 10 monomers. These sizes correspond to thicknesses from approximately 6 to 32 monomer diameters. Additionally, we simulate a pure bulk system at zero pressure that consists of 400 chains of 10 monomers each. All values are in reduced units where $\sigma_{\rm mm} = 1$ and $\epsilon_{\rm mm} = 1$, temperature in the units of ϵ/k_B (k_B is Boltzmann's constant), and time in unit of $\sqrt{m\sigma^2_{\rm mm}/\epsilon_{\rm mm}}$, where m is the monomer mass. In physical units relevant to real polymer materials, $\epsilon \approx 1$ kJ/mol for a polymer (like polystyrene) with $T_g \approx 100$ °C, the time unit is measured in ps, and the length of a chain segments σ is typically about 1-2 nm.

We use rRESPA multiple timescale integration method to improve simulation speed with $\delta t = 0.006$ [69]. Molecular dynamics simulations are performed in the canonical (NVT) ensemble (fixed number of particles, volume, and temperature). To prepare a supported film, we melt a crystalline polymer film confined in two impenetrable walls at a high temperature $T = 5.0$, until the crystalline polymer turns to an amorphous polymer melt. We then remove one of the wall to create a free-interface resulting a film with one attractive supporting wall (substrate). To obtain simulation data, we simulate all systems in a temperature range $T = 1.0$-

0.35, controlled by Noose-Hover method [66]. This temperature range covers both Arrhenius ($T > 0.6$) and non-Arrhenius behavior. In physical units, our lowest simulation temperature corresponds to a temperature where relaxation times $\tau \sim$ 1-10ns. For each temperature T polymer films are equilibrated for a running time roughly 100 times of the relaxation time to avoid non-equilibrium effects and to ensure the polymer melt is not in a crystalline state.

Chapter 3

Structural and Dynamical Properties of Polymer Films

In this chapter, we first examine structural changes in films, since free volume layer (FVL) suggests a connection between changes in dynamics and density. We start by examining the T-dependence of density ρ and film thickness h followed by evaluating the pair correlation function and structure factor. For dynamical analysis, we first describe the correlation function used to evaluate relaxation time in glass forming liquids and the T-dependence of relaxation time. Lastly, we describe the string-like cooperative motion in glass formers.

3.1 Structural Properties

3.1.1 Temperature Dependence of Density and Film thickness

We first examine density profile $\rho(z)$, shown in figure 3.1(a). Near the solid substrate ($z = 0$), we see strong density oscillations induced by the planar wall and

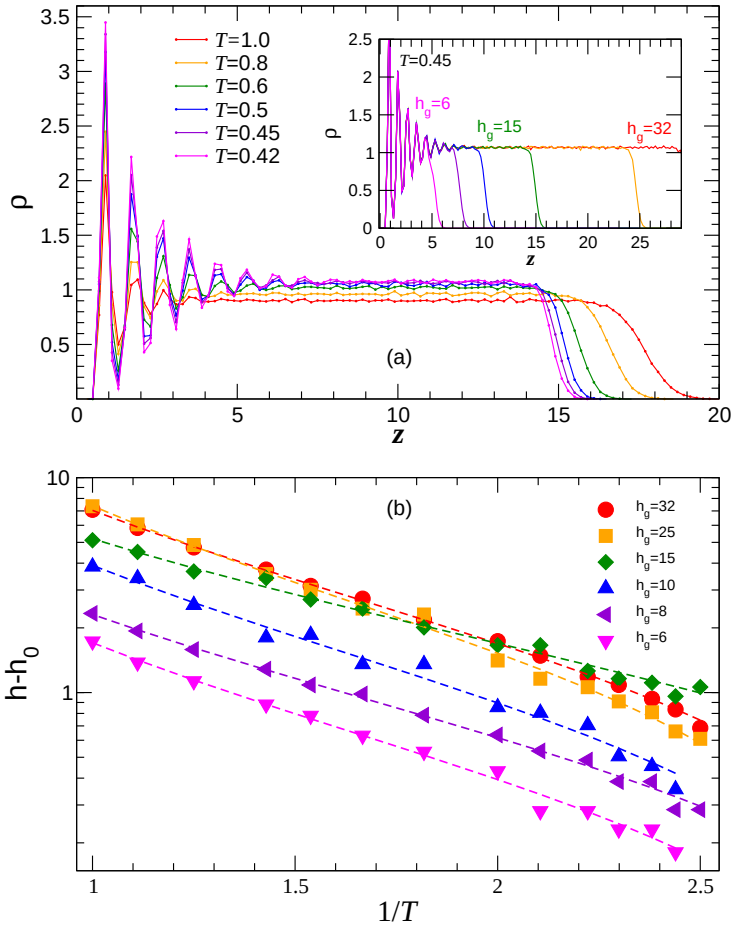

Figure 3.1: (a) Representative monomer density profile of $\rho(z)$ using a bin size $\delta z = 0.05$ for a supported film on a attractive surface for a range of T for film thickness $h_g = 15$, corresponding to about 30 nm in physical polymer units. It is apparent from $\rho(z, T)$ that the thickness of the film decreases on cooling. The inset shows density profile of monomer for various thicknesses scaled by the bulk value. We see that the peaks are independent of film thickness and there is a bulk like region far from the interfaces. (b) Temperature dependence of film thickness. Thickness h is plotted relative to its low temperature limit h_0, which demonstrates approximate Arrhenius behavior. We use this Arrhenius behavior to estimate $h(T_g)$.

a relatively more narrow and diffuse interface near the polymer free surface, just as anticipated by the layer model. Upon cooling, the film thickness decreases, the

overall density increases, the amplitude and the range of ρ oscillations near the solid substrate increase, and the polymer free-surface interface becomes progressively sharper (see figure 3.1). Based on the FVL model, $\rho(z)$ suggests slowed dynamics near the substrate, accelerated dynamics at the free surface, and a similar scale for the range of density and dynamical changes.

We precisely define the film thickness $h(T)$ from this density profile. Specifically, we define film thickness $h(T)$ as a distance from the substrate where $\rho(z)$ profile goes to 0.10. Other reasonable cutoff or using a fitting function [39] does not affect our qualitative findings. The resulting $h(T)$ [Figure 3.1(b)] is well described by an Arrhenius form

$$h(T) - h_0 = \Delta e^{-E/T}. \tag{3.1}$$

We extrapolate the Arrhenius fit to $T = T_g$ (determined from the dynamics described Chapter 4) to define the characteristic film thickness $h_g \equiv h(T_g)$[1].

3.1.2 Pair Correlation Function $g(r)$

The pair correlation function (or the radial distribution function) $g(r)$ describes the variation of density within a distance r from a reference particle. Mathematically, $g(r)$ is defined as

$$g(r) = \frac{V}{4\pi r^2 N^2}\Big[\sum_i \sum_j \delta(r - r_{ij})\Big]. \tag{3.2}$$

In films, it is useful to evaluate the pair correlation function in the direction parallel to the substrate, i.e. $g(r^{||})$, as a function of distance z from the substrate. Hence, we write

$$g(r^{||}) = C\Big[\sum_i \sum_j \delta(r^{||} - r_{ij}^{||})\Big], \tag{3.3}$$

[1]In figures, reported values of h_g are rounded to the nearest integer values.

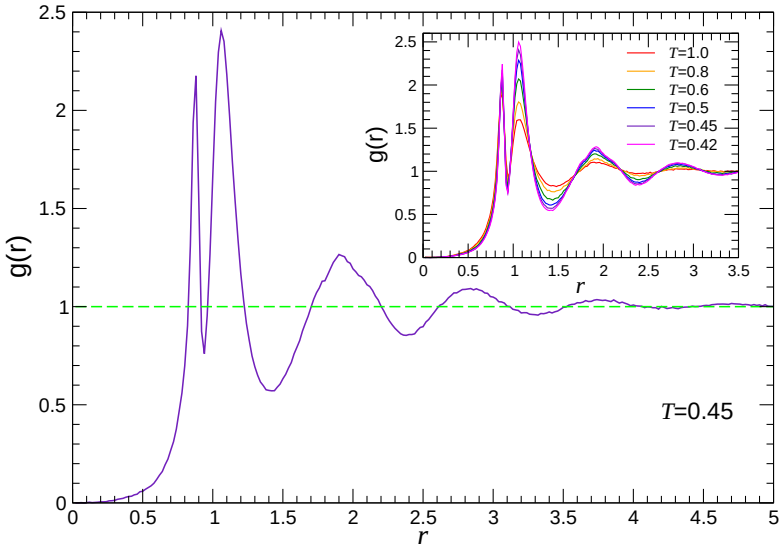

Figure 3.2: Pair correlation function $g(r)$ of a film with thickness $h_g = 15$ at $T = 0.45$. Inset shows $g(r)$ for various temperatures ranging from $T = 1.0$ to $T = 0.42$.

where C is a geometry-dependent normalization factor. In this section, we will only show the T-dependence of $g(r)$ for a film supported in a rough surface. In Chapter 5, we will use $g(r^{||}, z)$ extensively to examine local properties films supported on different surfaces.

Figure 3.2 shows (i) $g(r)$ vanishes as $r \to 0$ due to the exclude volumes between particles (ii) $g(r) \to 1$ with small oscillations at large r due to the weak long-range order particle interaction. The oscillatory behavior becomes more prominent for low T, as particles pack closer at lower T. The first peak of $g(r)$ locates the nearest neighbor. For particularly low $T < 0.6$, $g(r)$ exhibits two peaks that are close to each other at around $r = 1$. The first peak corresponds to the bonded-interaction (with an equilibrium distance at $r = 0.9$) and the second peak

corresponds to the non-bonded Lennard-Jones interaction (with an equilibrium distance at $r = 2^{1/6}$).

3.1.3 Structure Factor $S(q)$

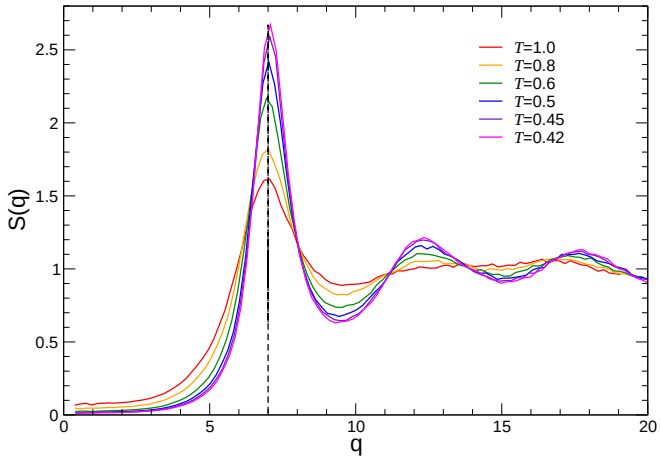

Figure 3.3: Structure Factor $S(q)$ of a film thickness $h_g = 15$. $S(q)$ becomes sharper as we decrease temperature. The peak is located at $q = 7.0$, which corresponds to the scale of first neighboring. Sharpening in $S(q)$ indicates increases in ordering in the liquid.

$g(r)$ is often determined indirectly via its relation to the structure factor function $S(\vec{q})$. This is so, because $S(\vec{q})$ can be measured experimentally using neutron or X-ray scattering. $S(\vec{q})$ is defined as time-independent density-density correlation function, which is proportional to the scattering intensity. As a first step, we write the particle density function in position space as

$$\rho(\vec{r}) = \frac{1}{N} \sum_j \delta(\vec{r} - \vec{r_j}), \tag{3.4}$$

of which we can take Fourier transform and obtain

$$\rho(\vec{q}) = \frac{1}{N}\sum_{j} e^{-i\vec{q}.\vec{r_j}}, \tag{3.5}$$

which is now in a momentum space. Since, as mentioned perviously, $S(\vec{q}) = \left\langle \rho^*(\vec{q})\rho(\vec{q}) \right\rangle$, we obtain

$$S(\vec{q}) = 1 + \frac{1}{N}\sum_{j\neq k} e^{-i\vec{q}.[\vec{r_j}-\vec{r_k}]}. \tag{3.6}$$

where we split the double sum into $j = k$ part and $j \neq k$ part. Replacing the sum in equation (3.6) with the integral, together with density correlation function $g(r)$ we obtain the desired relation between structure factor $S(\vec{q})$ and the correlation function $g(r)$ as

$$S(\vec{q}) = 1 + \rho\int_{V} e^{-i\vec{q}.\vec{r}} g(r), \tag{3.7}$$

In an ideal gas system with no interaction, $S(\vec{q}) = 1$ for all $\vec{q}$, as the second term of equation (3.6) equals to zero. Liquids are isotropic, thus we need not examine the vector dependence, and focus only on the magnitude $q = |\vec{q}|$. In our polymeric liquid, $S(q)$ has a peak at $q = 7.0$, shown in figure 3.3. This peak corresponds to the length scales of the first neighboring as observed in $g(r)$ (see figure 3.2). Figure 3.3 shows that intensity of $S(q)$ increases with decreasing T indicating that particles become more ordered. Measuring $S(q)$ is important in our analysis because we can check occurrence of crystallization (high periodicity). If in crystalline state, sharp peaks should be observed in $S(q)$.

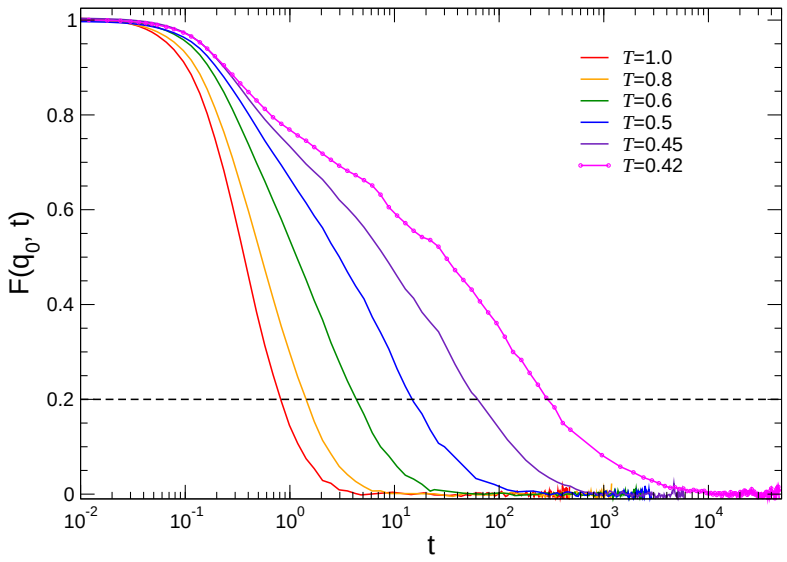

Figure 3.4: Coherent Intermediate Scattering Function $F(q_0, t)$. $F(q_0, t)$ shows exponential decay at high T. At low T, two step relaxation occurs where $F(q_0, t)$ no longer can be expressed in simple exponential decay. The first relaxation correspond to vibrational relaxation and the other relaxation corresponds to diffusive relaxation.

3.2 Dynamical Properties

3.2.1 Intermediate Scattering Function $F(q, t)$

To characterize the dynamics in polymer films we evaluate a characteristic time τ, a time scale where in equilibrium the system is fully relaxed structurally. We quantify this time scale using Intermediate Scattering function (ISF). The ISF is defined as time-dependent density-density correlation function given by

Roughly speaking, ISF measures the time evolution of liquid's structure. For-

mally, ISF [denoted by $F(q,t)$] is given by

$$F(q,t) \equiv \frac{1}{N}\Big\langle \rho^*(\vec{q},t)\rho(\vec{q},0)\Big\rangle. \tag{3.8}$$

where N is the particle number. Using definition of $\rho(\vec{q})$ from equation 3.5 with additional time factor we can write

$$F(q,t) \equiv \frac{1}{NS(q)}\left\langle \sum_{j,k=1}^{N} e^{-i\vec{q}.[\vec{r}_k(t)-\vec{r}_j(0)]} \right\rangle, \tag{3.9}$$

where $\vec{r}_k(t)$ is the position of the particle k at time t and $\vec{q}$ is the wave vector. $S(q)$ is the structure factor given by equation (3.6) and so that at $t = 0$, $F(q,t)$ is normalized to 1. Specifically, we choose $|q| = q_0$, where $q_0 = 7.0$ is the peak of $S(q)$. Choosing q_0 with the highest periodicity results largest relaxation time since the de Gennes narrowing hypothesis tells us that $\tau(q) \sim S(q)/q^2$. Specifically, we define the characteristic time τ by $F(q_0,\tau) = 0.2$.

Figure 3.4 shows $F(q_0,t)$ of film thickness $h_g = 15$ for various temperature. At high temperature, $F(q_0,t)$ can be expressed as a simple decaying exponential function, which is commonly observed in simple liquids. At low temperature $F(q_0,t)$ exhibits a two step relaxation. The first step relaxation is commonly related to vibrational relaxation and the second one is commonly related to structural relaxation. The structural relaxation can be expressed as a stretched exponential function,

$$F(q,t) \sim \exp\Big[-(t/\tau)^{\beta}\Big], \tag{3.10}$$

where β typically ranges from 0.3 to 1.0. This two step relaxation is often associated with "caging" of monomers , a scenario in which a particle being trapped by its nearest neighbor. Several studies have indicated that β can be related to fragility in glass forming liquid [70, 71]. However, in this thesis, we will not examine β in relation to the glass formation. We instead study the glass transition

and fragility from the cooperative behavior of monomers within the films. The temperature dependence of τ will still be discussed in Section 3.2.3.

3.2.2 Incoherent Intermediate Scattering Function $F_{\mathrm{self}}(z, q, t)$

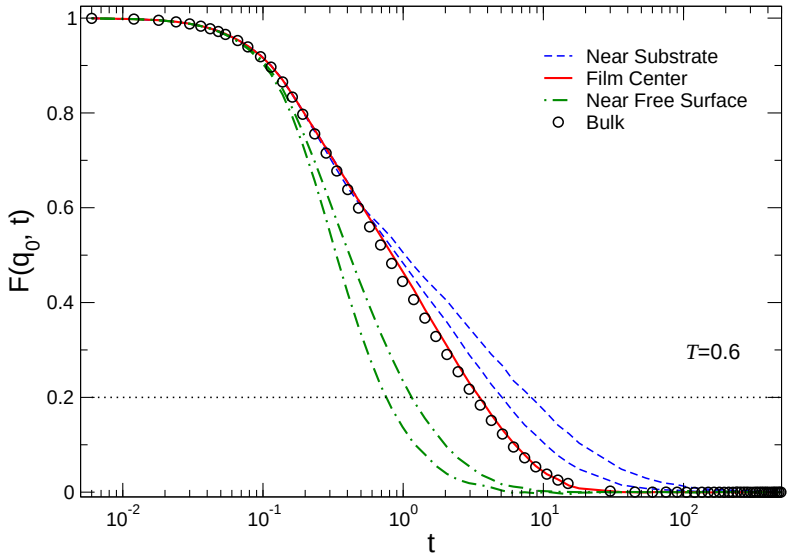

Figure 3.5: $F_{\mathrm{self}}(z, q_0, t)$ of film thickness $h_g = 15$ at $T = 0.6$ decomposed into layers as a function of distance z from the supporting substrate. Specifically, we decompose films into layers with a width $\delta z = 0.875$ based on layering density profile. In substrate region with a relatively strong interaction, monomers are relaxed much slower than the film center. In contrast, at the free-surface, monomers are diffused relatively much faster than the film center. Monomers at film center, where monomers are not perturbed by surfaces, relax closely to the bulk's relaxation.

Films are highly heterogenous due to interfacial effects, and, therefore, it is useful to evaluate the dynamics locally. We use the self or incoherent $F_{\mathrm{self}}(z, q, t)$ part (i.e. $j = k$) of equation (3.9), on the basis of the position z of a monomer at

$t = 0$. We define the relaxation time $\tau_s(z)$ by $F_{self}(z, q_0, \tau_s) = 0.2$.

We evaluate $F(q_0, t, z)$ of films with the partitioning interval $\delta z = 0.875$ for all temperatures based on the layering density profile [see figure 3.1(a)]. Smaller or larger value of δz does not affect our qualitative findings. Figure 3.5 shows the typical $F_{self}(q_0, t)$ within the film. Near the free surface, monomers are relaxed much faster in comparison to the film center which is close to the bulk relaxation. In contrast, near the rough surface monomers relaxed at a greater time indicated by the two-step relaxation process.

3.2.3 Temperature Dependence of Relaxation Time τ and Glass Transition temperature T_g

In a simple liquid, the T dependence of τ is usually described by the Arrhenius equation,

$$\tau(T) = \tau_0 \exp\left[\frac{\Delta G}{k_B T}\right], \tag{3.11}$$

or Eyring equation [72]. In the transition state theory, ΔG is the free energy of activation, the required energy for a particle to relax into another configuration. In the glass forming liquid, this Arrhenius behavior no longer holds at temperatures below an onset temperature called Arrhenius temperature, T_A.

In this non-Arrhenius behavior regime, many unusual behaviors have been observed such as the occurrence the two-step relaxation of the ISF and the particle clustering [49, 55, 73]. Many theories have been proposed to explain this 'super Arrhenius' behavior such as MCT [70, 71] and AG theory [47]. The non-exponential growth of τ in many glass-forming liquids can be described by the empirical Vogel-Fulcher-Tammann (VFT) equation,

$$\tau(T) = \tau_0 e^{DT_0/(T-T_0)}, \tag{3.12}$$

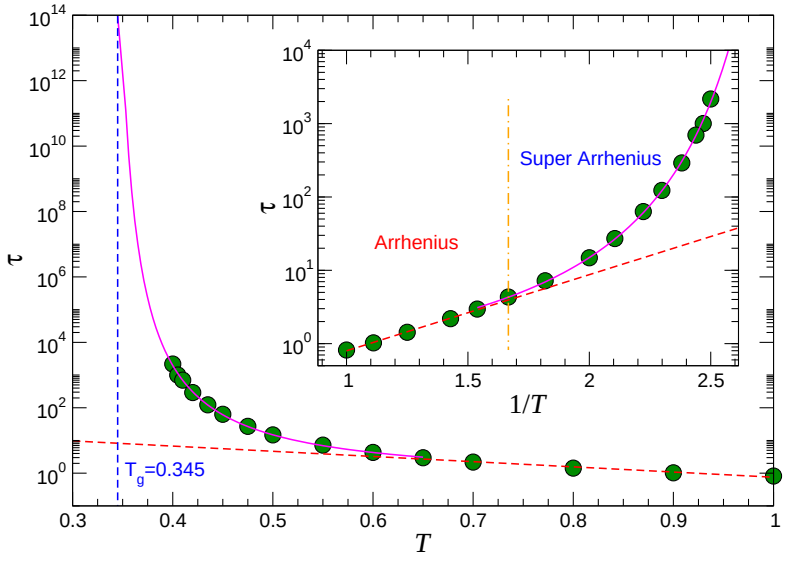

Figure 3.6: Temperature dependence of relaxation time $\tau(T)$ of a film with thickness $h_g = 15$. The symbols represent simulation data, dotted red and solid line represent the fitting using the Eyring equation (3.11) and the VFT equation (3.12). Inset shows the Arrhenius behavior of τ above $T_A = 0.6$. Below T_A, T-dependence of τ transition into 'super Arrhenius' behavior which is well described by the VFT equation (3.12).

where T_0 is the temperature where τ diverges on extrapolation.

In experiments, T_g is often defined as T at which the relaxation time reaches 100s [9], and we adopt this simple criterion here. Specifically, we fit our simulated data for $T_0 < T < T_\mathrm{A}$ to the equation (3.12) to obtain extrapolated value $\tau = 100s$. Figure 3.6 shows how the T dependence of τ is well described by VFT equation (3.12) for $T < T_\mathrm{A} = 0.6$ and by the Arrhenius equation (3.11) for $T > T_\mathrm{A}$.

3.2.4 Fragility m

As noted earlier, the breadth of glass transition temperature varies for different glass formers. T_g itself does not provide enough information for comparing changes in dynamics toward T_g of different glass formers. Therefore, in order to study glass-formation, we also need to evaluate fragility m defined as the rate of change of relaxation time (or viscosity) as a function of temperature. We use the most common definition of fragility defined as the slope logarithm of the relaxation time at temperature T near T_g

$$m(T_g) = \left.\frac{\partial \ln \tau}{\partial (T/T_g)}\right|_{T_g}. \tag{3.13}$$

We evaluate fragility m using the fit of equation (3.12). Using equation (3.12), we obtain an explicit expression of m

$$m(T_g) = \left.\frac{DT}{(T-T_0)^2}\right|_{T_g}. \tag{3.14}$$

For film thickness $h_g = 15$ supported on a rough surface, we obtain $D = 1.80$, $T_0 = 0.328$, and $\tau_0 = 0.494$. And according to equation (3.14), we found the estimated fragility to be $m = 635$. Experimentally m is often found to be proportional to T_g for polymers [74]. However, measuring fragility in more detail becomes important in analyzing polymer films, because competing effects between substrate and free-surface may result in a non-monotonic dependence of thickness on overall T_g and m. That is, at some critical thickness where interfaces are dominant, T_g and m is no longer proportional to each other [39].

3.2.5 String-Like Cooperative Motion

Glass formers are dynamically heterogenous, typically manifested by spatial correlations of mobility. Several studies have found the existence of cluster formation

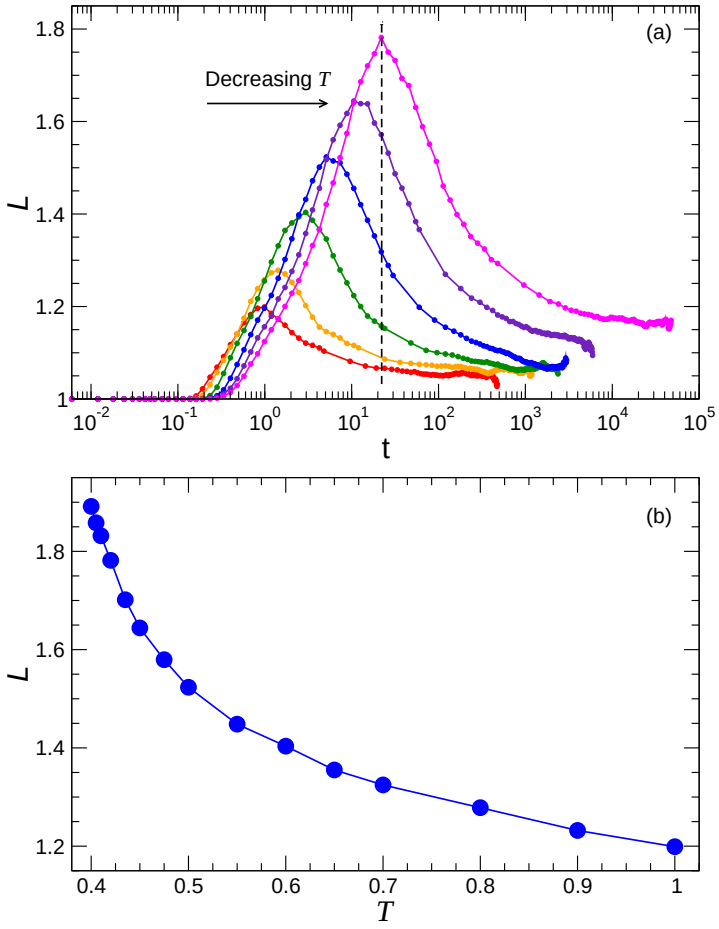

Figure 3.7: (a) Average strings length $L(t)$ of film thickness $h_g = 15$ for various T. The peak of $L(t)$ and the characteristic time t required for monomers to form the longest average strings length increases with decreasing T. (b) Temperature dependence of the of peak of $L(t)$.

of the most mobile particles, and the found that subsets within these clusters move in quasi-one-dimensional path replacing one another in a string-like fashion [47, 56–59, 75]. Studied by Ref. [55], mobile particles in our system typically account 5-7% of particles below T_{A}. Accordingly, following Ref. [55] we select most mobile particles as 6.5% of the particles with greatest displacement over time t.

Significantly, several works [55, 60, 61, 76] indicate that this string size may offer a molecular realization of CRR. Accordingly, we evaluate the average size of string-like cooperative motion, $L(T)$. We evaluate $L(T)$ following the methods described in Ref. [50, 55]. Specifically, mobile particle i and j are considered to be in the same string if

$$\min\left[|\vec{r_i}(t) - \vec{r_j}(0)|\right] \text{ and } \min\left[|\vec{r_j}(t) - \vec{r_i}(0)|\right] < \delta. \tag{3.15}$$

This is to say, if particles i and j satisfy the conditions in equation (3.15), the particle i moves from $\vec{r_i}(0)$ to $\vec{r_i}(t)$ in time t, while the other particle j moves from to $\vec{r_j}(0)$ to $\vec{r_j}(t)$ within a radius δ. Specifically, we choose $\delta = 0.3025$ to avoid unambiguous replacement [50].

Figure 3.7 (a) shows the time-dependent of average strings length $L(t)$ of film thickness $h_g = 15$ for various T. $L(t)$ exhibits a maximum for each temperature; the time required to reach this maximum as well as the value of this peak grow with decreasing temperature [shown in figure 3.7(b)]. The growth of average strings length upon cooling implies increasing cooperativity is at work in actualizing the growth of CRR, supporting arguments proposed by Adam and Gibbs [47].

Chapter 4

Glass Transition and Fragility in Polymer Films

In this chapter we examine the T dependence of overall dynamics characterized by relaxation time τ for films with various thicknesses supported on rough or smooth surfaces. Then, we contrast the thickness dependence of T_g and m on films supported on a rough and smooth surface. Further, we examine the overall changes in τ of films with variation in polymer-substrate interaction ϵ_{wm} and surface rigidity k. Lastly, we evaluate the surface factor (ϵ_{wm} and k) dependence of T_g and m and see how film thickness can complicate both the resulting T_g and m.

4.1 Thickness Dependence of T_g and m on Films on Rough vs. Smooth Surfaces

In this section, we investigate the overall changes that occur in glass formation process of polymer films supported on the rough or smooth substrate. Specifically,

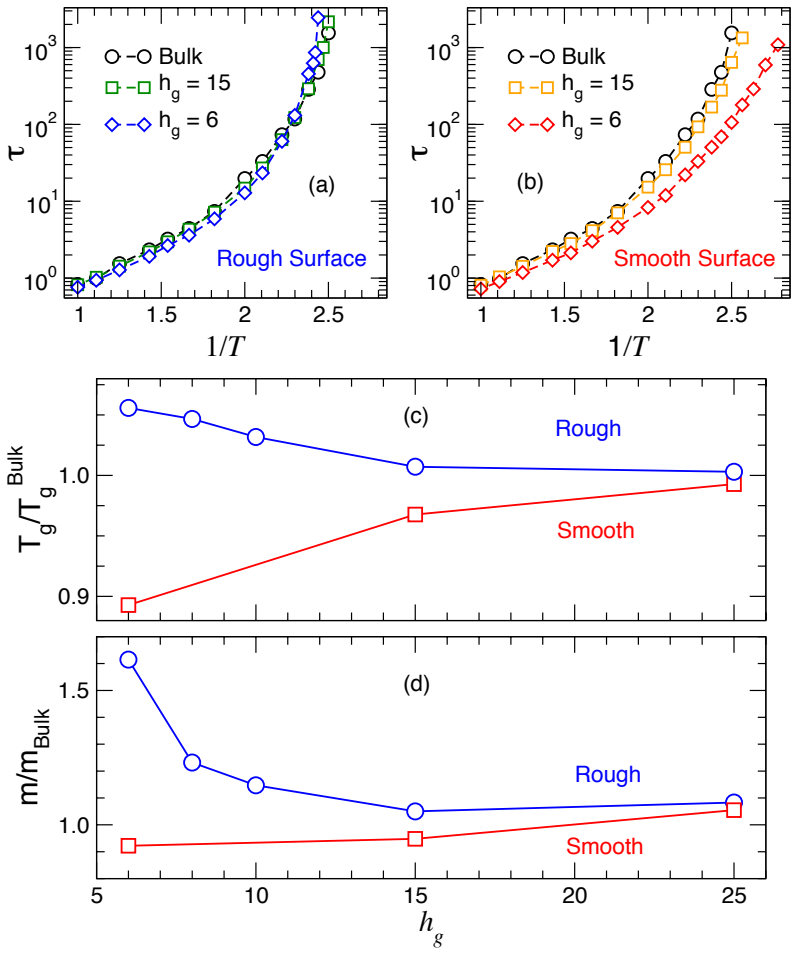

Figure 4.1: Effects of film thickness and structure of the supporting surface on glass transition temperature T_g and fragility. The T dependence of relaxation time τ of a bulk system and two representative film thicknesses supported on a rough (a) or smooth (b) surface. In this T range, it is apparent that relative to the bulk τ increases as we decrease the thickness of the film supported on rough surface relative to the bulk, while films supported on smooth surface shows an opposite behavior. (c) Relative T_g and (d) fragility m to the bulk as function of film thickness. Both T_g and m of films supported on rough surface increases while T_g and m of smooth surface decreases as we decrease film thickness.

we vary the thickness of the polymer film, where the supporting wall shares the same wall-monomer interaction ($\epsilon_{\rm wm} = 1.0$). The main focus will be to discuss the differences between the smooth and the rough surfaces.

Relative to the bulk system, the relaxation time τ of polymer films on the smooth surface decreases as we decrease film thickness, and these deviations become more pronounced as we go to lower T, consistent with previous studies [38, 39] [see figure 4.1(b)]. However, we find an opposite behavior for the rough surface, as noted in Ref. [77, 78]. We see that the dynamics change more rapidly with T for thinner films resulting in a higher relaxation time relative to the bulk system [see figure 4.1(a)]. Importantly, the roughness of the surface alters the overall dynamics, even for identical wall-monomer interaction strength for the smooth and rough surfaces. We estimate T_g by fitting our data with Vogel-Fulcher-Tammann (VFT) equation in equation (3.12). We adopt the commonly defined T_g as as T at which the relaxation time reaches 100s [9]. Figure 4.1 (c) shows that, relative to the bulk, T_g of polymer films on the rough surface increases with decreasing film thickness, while for the smooth surface systems, T_g decreases with decreasing film thickness.

The variation in T dependence of relaxation is quantified by fragility m [see equation (3.13)]. We evaluate fragility m using the fit in equation (3.12). In figure 4.1(d), we see that relative to the bulk, films on rough surface become more fragile as we decrease thickness, which is apparent from the increasingly rapid variation of $\tau(T)$ [figure 4.1(a)]. In contrast, the fragility of polymer films on the smooth surface increases with decreasing film thickness.

Experimentally, T_g is often found to be proportional to m [74]. We also find a correlation between T_g and m for both surfaces, but this relation is not strictly proportional. Note that the films supported on a smooth surface may have a non-monotonic thickness dependence of T_g and m on thickness. Specifically, our

recent work [39] showed that T_g or m decreases with decreasing film thickness up to some critical thickness, but then T_g increases for very thin films as interfacial effects become dominant.

4.2 Dependence of T_g and m on Substrate Interaction and Surface Rigidity

Substrate roughness is clearly relevant to the film dynamics, but there are other evident relevant variables. We investigate the dependence of dynamics on the interfacial interaction strength as well as rigidity of the rough substrate. First, we examine the role of surface interaction strength. Figure 4.2 (a) and (b) show how relaxation time for two representative film thicknesses changes as we vary the interaction strength ϵ_{wm} between the rough wall and the polymers. The overall changes in dynamics result from the competing effects of the substrate and free interface, so that the relaxation time can be higher or lower compared to the bulk. As we have established before, the free surface decreases the relaxation time while a substrate with a relatively strong interaction increases relaxation time. Thus, for a given thickness, τ decreases with the decreasing interfacial interaction.

We find a similar effect when varying the stiffness k of the bonds describing the substrate stiffness. Specifically, increasing the flexibility of the substrate atoms (decreasing k) results in a smaller τ [figure 4.2 (c) and (d)]. Evidently, monomers near the wall are less constrained, since the substrate atoms are more flexible. The complete local analysis of the dynamics will be discussed in Chapter 5. By comparing figure 4.2 (a) and (b) as well as (c) and (d), we can clearly see that the surface interaction or the flexibility of the substrate have greater influences on the thinner film, which is expected since the thinner film has a bigger interfacial

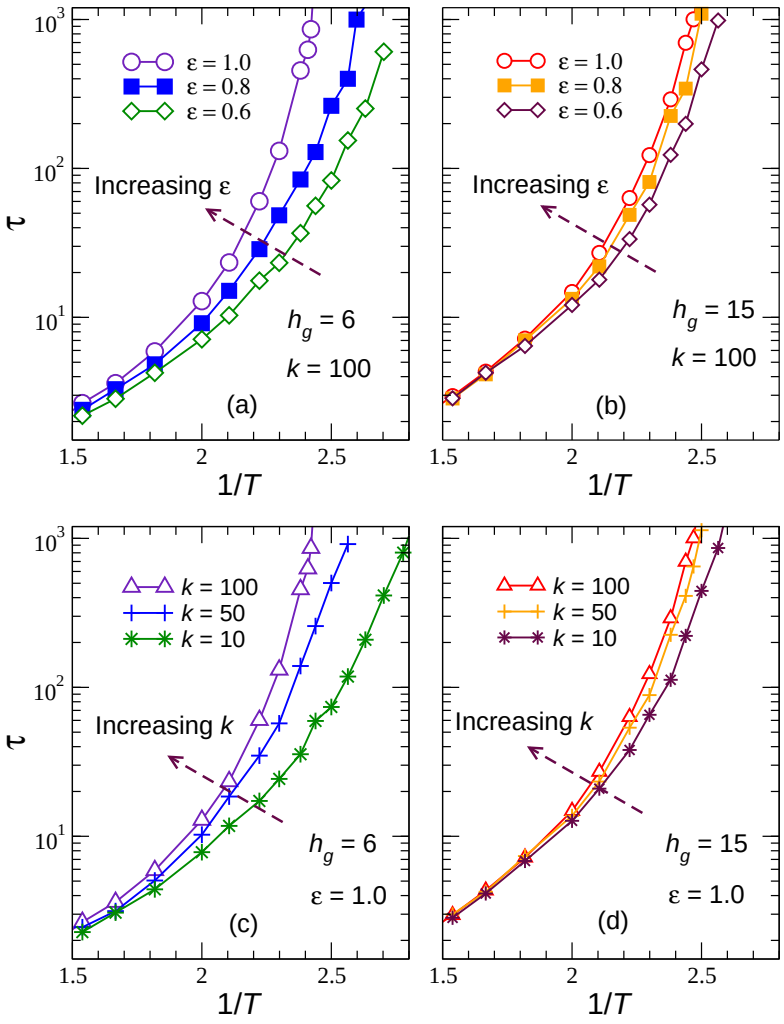

Figure 4.2: The T dependence of the relaxation time τ of two film thicknesses, h_g=15 and 6, with various interfacial strength $\epsilon_{\rm wm}$ [(a) and (b)] and the flexibility of the wall atoms k [(c) and (d)]. In general, dynamics are enhanced as we decrease the interfacial strength or the molecular-wall stiffness.

surface-to-volume ratio.

We next evaluate the resulting dependence of the glass transition temperature T_g and fragility m on the interfacial interaction strength and rigidity of the rough

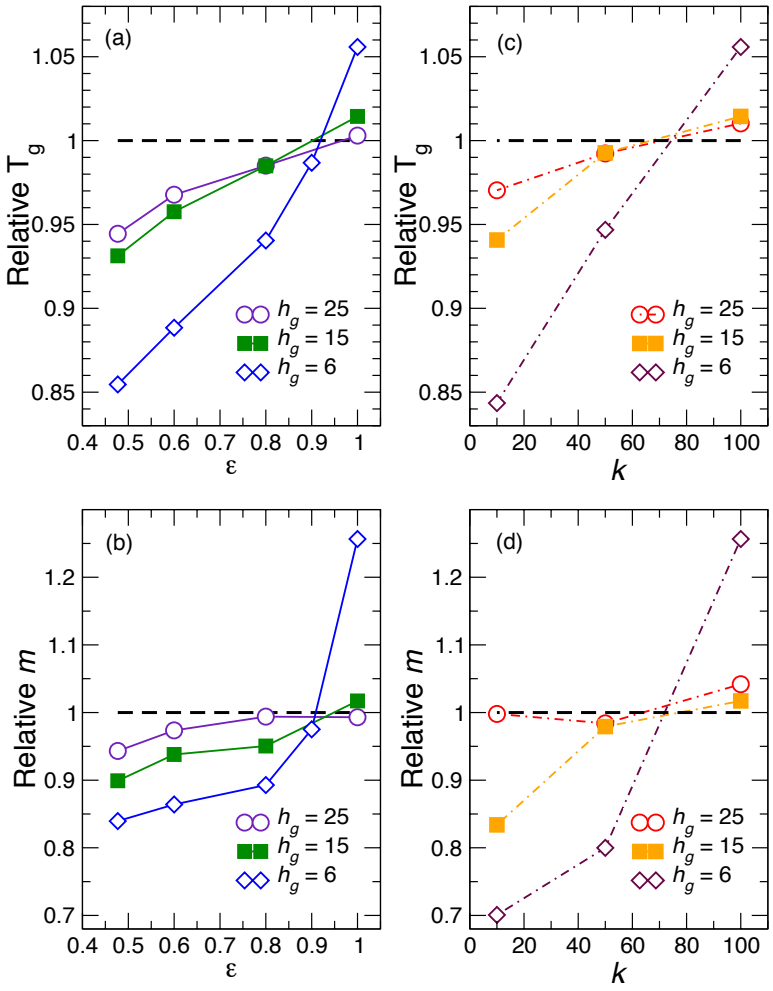

Figure 4.3: Dependence of the relative T_g and m of three representative film thicknesses on interfacial strength $\epsilon_{\rm wm}$ ((a) and (b)) and surface rigidity k ((c) and (d)). For thinner films, the range of T_g and m is wide due to the larger surface ratio.

surface. Figures 4.3 (a) and (b) show how T_g of three representative thicknesses change with varying surface interaction $\epsilon_{\rm wm}$ at a fixed rigidity $k = 100$. Generally, increasing the polymer-substrate interaction increases both T_g and m as monomer dynamics near the surface presumably become progressively slower. These gen-

eral trends of a decreasing T_g with decreasing interfacial interaction have also been observed both in experiments and computational works [18, 24, 64, 65]. This depression of fragility is also consistent with the findings in a free-standing film [27], which formally takes $\epsilon_{\rm wm} \to 0$. Clearly, the dependence of T_g or m on the surface polymer interaction becomes more significant for thinner films, indicated by a steeper variation of T_g or m with $\epsilon_{\rm wm}$, as shown in figure 4.3.

We found similar trends of T_g and m for varying substrate rigidity. That is, increasing surface rigidity k at fixed substrate interaction strength ($\epsilon_{\rm wm} = 1$) increases both T_g and m. It is interesting to note that there appears to be a nearly fixed point for T_g and m as function of $\epsilon_{\rm wm}$. Specifically, for $\epsilon \simeq 0.9$ ($k = 100$) or $k \simeq 75$ ($\epsilon_{\rm wm} = 1$) T_g and m, are independent of film thickness. We emphasize that this does not mean there is no change in local dynamics, but rather that there is a precise balance between the dynamic enhancement at the free surface and the slowing down of the dynamics at the substrate. This finding is reminiscent of compensation effect of the self-excluded volume interaction of polymers in solution near the theta point, where the measured properties of polymer become independent of the solvent.

Both results potentially offer us insights into how T_g changes in multilayer films, which are "stacks" of polymer films with different species characterized by different flexibility, inter-polymer interaction, or molecular weight (different T_g). Multilayer films experiments by Torkelson and co-workers have shown that different layers within a multilayer may have different T_g depending on the properties of neighboring layers [46]. Here we emphasize that changes in dynamics do not necessarily arise from the interfacial interaction strength alone; changes in the rigidity of the interface (e.g polymer films placed on polymer substrate having same interaction, but having different molecular flexibility which is commonly characterized by different T_g) and interfacial roughness introduced in fabricating

the polymer layers are also potentially relevant.

Chapter 5

Local Structural and Dynamical Changes in Polymer Films

In Chapter 4, we have already shown that the overall dynamics of polymer films, characterized by the glass transition temperature T_g and m, can be altered significantly by changing relevant variables such as, film thickness, surface roughness, interfacial interaction strength and surface rigidity. Conceptually, any local changes in dynamics contribute the overall changes. We should be able to understand the dependence of the relevant parameters on T_g and m by examining the local dynamics. In particular, free volume layer (FVL) picture suggests a connection between changes in structure (i.e density) and in dynamics.

Specifically, in this chapter we examine the local changes in structure and dynamics for film with various thicknesses supported on a rough or smooth surface, as well as films supported on substrates with different surface interaction ϵ_{wm} and surface rigidity k. We show that no significant changes is observed in structure, evidenced in the monomer density and pair correlation function analysis, despite great changes is observed in film dynamics characterized by relaxation

time obtained via Intermediate Scattering Function. This results suggests that free volume layer picture is inadequate in explaining changes in dynamics. Further, by obtaining local relaxation time within the films we are able to evaluate T_g and fragility m variation in polymer films.

5.1 Structural Changes

To understand the observed overall changes in T_g and fragility m, we resolve both structure and dynamics locally, since the changes in the film as a whole should be manifested by its local properties. The details of the analysis measuring monomer density ρ, pair density correlation function $g(r)$, and other relevant quantities can be found in Chapter 3.

We first contrast the local dynamics and monomer density as functions of distance z from the substrate boundary of rough or smooth surfaces with $\epsilon_{\mathrm{wm8}} = 1$. We evaluate both monomer density $\rho(z)$ and local relaxation time $\tau_{\mathrm{s}}(z)$ with a bin size $\delta z = 0.875$. In figure 5.1 (a), we observe that the monomer density near either surfaces increases slightly, and has a steady value through most of the film ($z \lesssim 13$). The density drops down to zero over a narrow window at around $z \sim 15 \pm 2$ transitioning to the free surface region. At the center of the film, the density has a value close to that of the bulk. We note that the density profile of the film on smooth surface is essentially identical to that of the film on rough surface.

This time, we investigate the local structure parallel to the substrate by evaluating the density pair correlation function $g(r_{||})$ [figure 5.1 (b) and (c)]. Far from the substrate, $g(r_{||})$ of both systems are identical as the monomers are completely unperturbed by the substrate, shown in figure 5.1 (c). Near the substrate [see figure 5.1 (b)] , we see that there is a slight difference in the local structure.

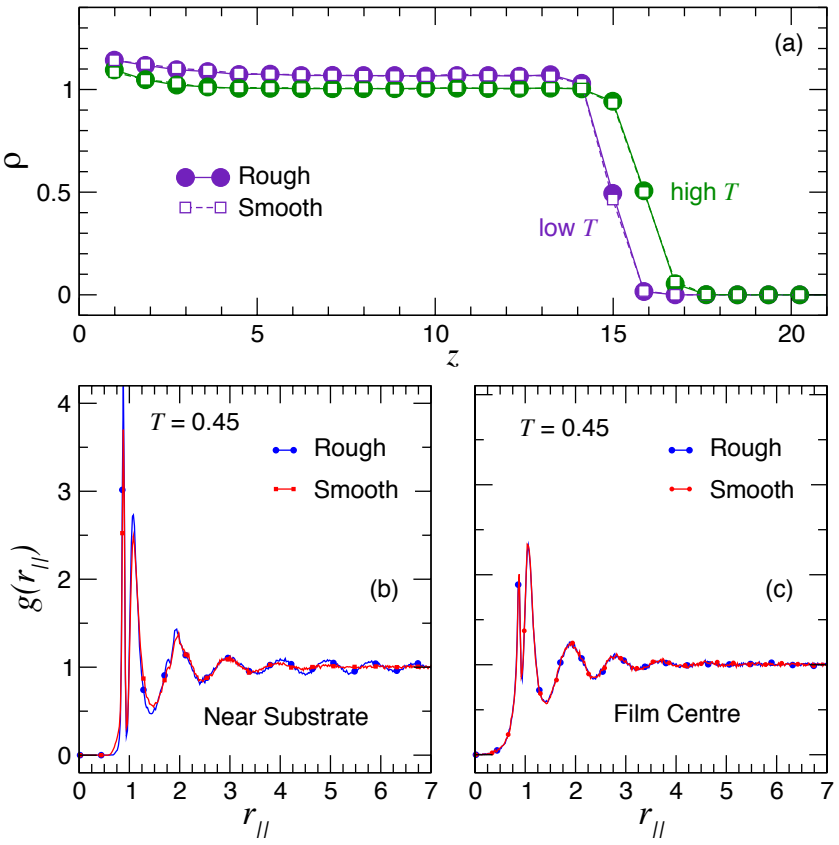

Figure 5.1: (a) Monomer density profile $\rho(z)$ of a film, $h_g = 15$, supported on rough or smooth surface using bin size $\delta z = 0.875$. Density pair correlation in parallel direction $g(r_{||})$ near the substrate (b) and at the film center (c). Near substrate $g(r_{||})$ between two surfaces show differences even though it is not significant. Monomers near the rough surface are slightly more packed and have better long-range ordering in comparison to those near the smooth surface.

Here, $g(r_{||})$ of the rough surface carries somewhat higher peaks, showing that the monomers near the rough surface are more ordered in comparison to those near the smooth surface. In addition, there is a weak long-range ordering of monomers for the rough surface, potentially induced by the periodicity of the wall atoms. Since the overall dynamics of rough and smooth substrates differ significantly, it

is clear that the free volume and structural based interpretations of T_g changes are inadequate.

5.2 Local Changes in Dynamics

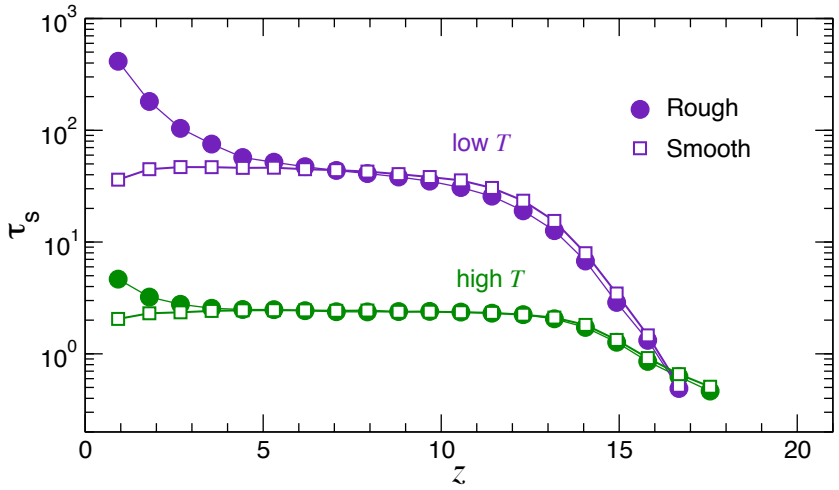

Figure 5.2: Relaxation time τ_s as a function of distance z from the substrate. Although the averaged densities of the two systems (rough and smooth surfaces) are identical, the local dynamics is clearly distinct from one another, particularly near the the substrate.

We next examine the local film dynamics. Figure 5.2 shows that the dynamics of the film on a rough or smooth surface are nearly identical from the center of the film to the free surface. However, there are large differences of relaxation time near the substrate. The local relaxation time τ_s increases close to the rough surface but decreases in the case of the smooth surface. The enhanced dynamics near the smooth surface is a consequence of the fact the monomers can "slide" along the substrate due to its smoothness (see Refs. [39, 79]). This effect is non-existent for a rough surface. In contrast, the relaxation time increases near a

rough surface, presumably because of a relatively strong interaction, as have been observed in a number of computational studies including those that investigated binary Lennard-Jones liquids or a bead-spring model of polymer melt [25, 26, 77, 78]. We, therefore, conclude that surface roughness is a decisive parameter for the polymer film dynamics. Hence, the surface roughness factor must be controlled carefully for consistent results.

5.3 Local Structure and Dynamics with Variation in Substrate Interaction and Surface Rigidity

We revisit our analysis of both film structure and dynamics to further confirm our arguments about the role of interfacial changes on the overall dynamics. Figures 5.3 (a) and (c) show how the monomer density $\rho(z)$ responds to the changes in the interfacial strength $\epsilon_{\rm wm}$ or rigidity k of the wall. Far from either substrate, $\rho(z)$ has a steady value close to the bulk. In general, the density near either substrate increases slightly as we increase $\epsilon_{\rm wm}$ or k. Only at very low rigidity ($k = 10$) we find considerable changes in the local density: $\rho(z)$ has a value close to the bulk value except at the region very close to the substrate. This most flexible wall, low rigidity, can be thought of as an amorphous solid wall that does not perturb the film much, because such a wall can adapt its structure to that of the deposited film.

Similar to our findings in comparing rough and smooth surfaces, we find substantial changes in local relaxation time $\tau_{\rm s}$ at the surface as a function of $\epsilon_{\rm wm}$ or k, despite no significant changes in the local density as $\epsilon_{\rm wm}$ and k are varied [see figure 5.3]. This again confirms the limitations of a free volume based interpre-

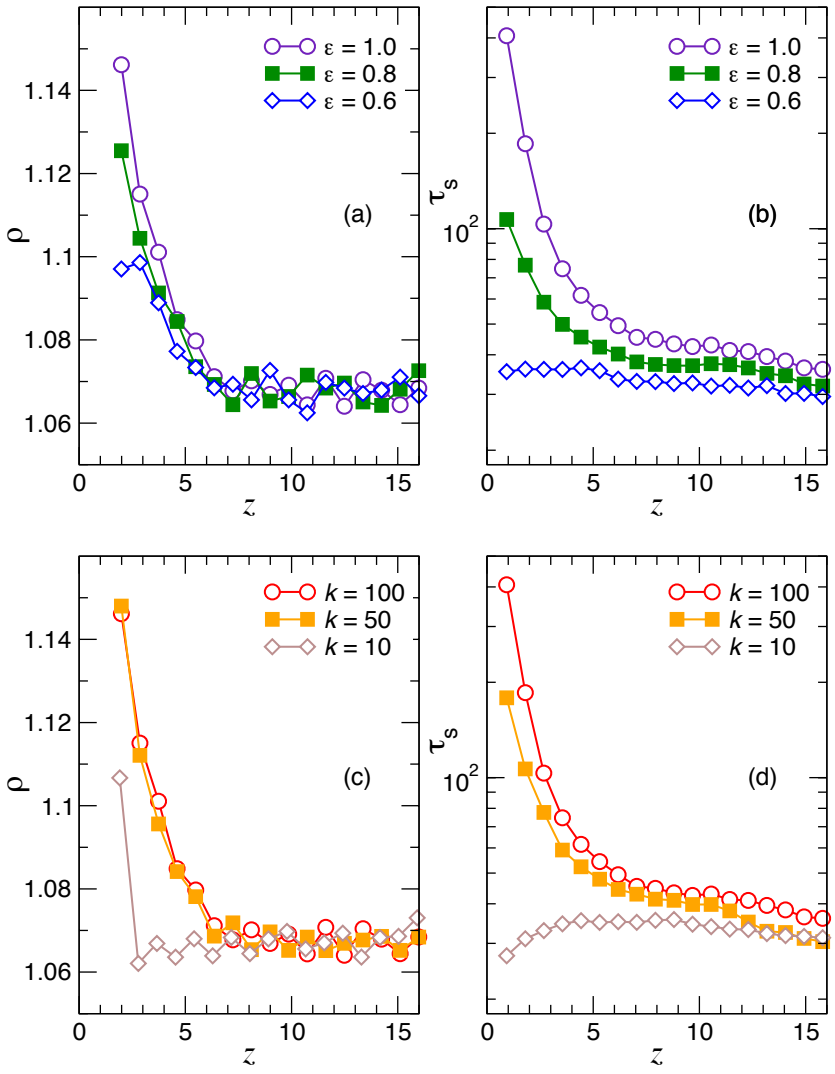

Figure 5.3: Variation monomer density profile $\rho(z)$ and local relaxation time τ_s as function distance z from the substrate with varying polymer-substrate interaction ϵ_{wm} ((a) and (b)) or surface rigidity k ((c) and (d)).

tation of thin film results. Local relaxation time $\tau_s(z)$ generally decreases as we decrease ϵ_{wm} or k. Weaker interfacial interaction allows monomer to avoid caging

near the attractive substrate. Likewise, decreasing wall rigidity allows monomers to move freely, since the wall atoms are not strongly localized.

5.4 Local T_g and fragility m

A convenient way to parameterize local dynamical changes is to use the local dependence T_g and m as functions of distance z from the substrate, based on T dependence of $\tau_s(z)$ [see figure 5.2]. We estimated $T_g(z)$ and $m(z)$ following the procedures described in Section 3.2.3 and 3.2.4. Figure 5.4 (a) shows that T_g increases near the substrate for rough films, reflecting the fact that τ_s increases near the attractive substrate. Near the free surface, T_g decreases due to the enhanced mobility of monomers at the free surface boundary. For relatively thick films, there is a substantial region in which T_g is close to that of the bulk value, a scenario where the film thickness is large compared to the perturbing scales of the interfaces [39]. T_g is often found to be proportional to m, as it is observed in the overall dynamics. However, we do not see this proportionality between the local T_g and m. Specifically, m *decreases* approaching the rough surface while T_g *increases*. This opposite trend has also been observed in polymer-nanoparticle composites [61].

Figures 5.4 (c) and (d) contrast the local variation of T_g and m for rough and smooth surfaces of a relatively thick film, $h_g = 15$. In contrast to the increasing T_g of polymer films near the rough substrate, T_g of smooth surface decreases as it gets closer to the smooth surface, which is consistent with our findings of variations of τ_s shown in figure 5.2. Note that T_g and m are depressed for films supported on the smooth surface, even at the middle of the film, a scenario where the perturbing scales of both interfaces become comparable to film thickness, meaning that effectively the entire film is affected by both interfaces.

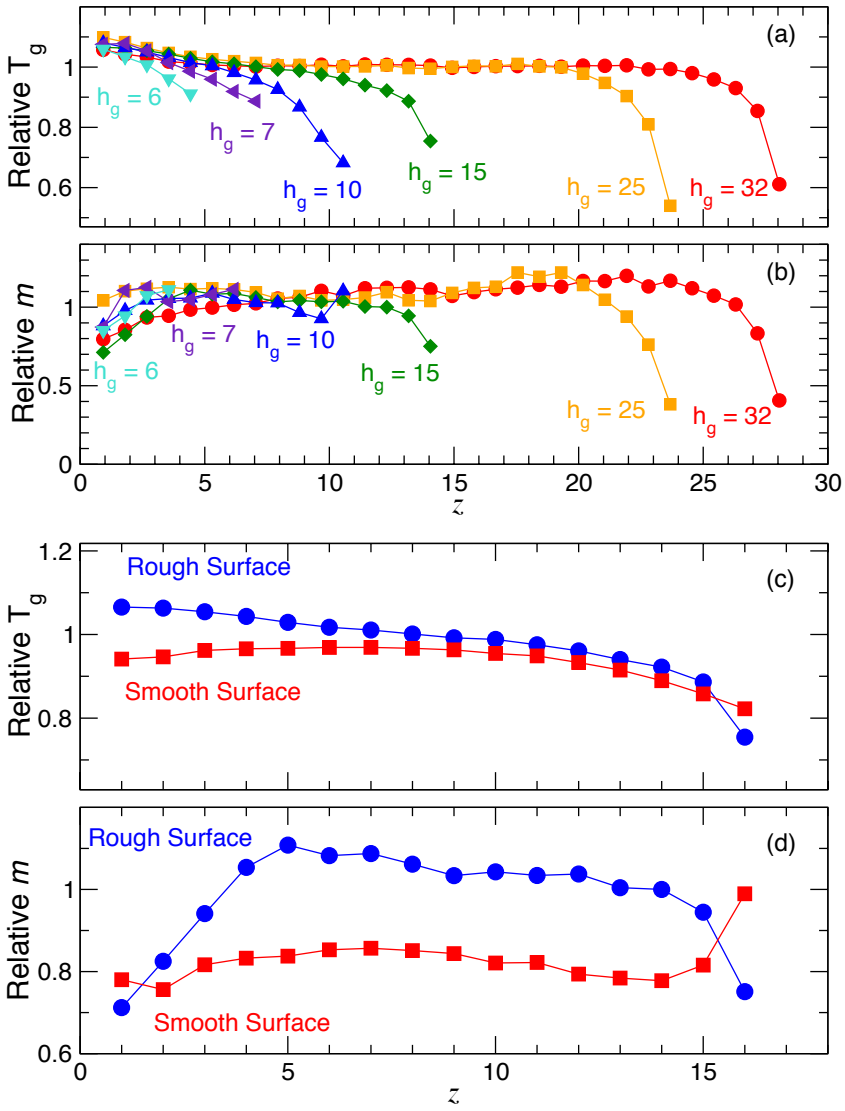

Figure 5.4: Local T_g and fragility m as a function distance z from substrates. Shown in (a) and (b) are the glass transition temperature T_g and the fragility m, respectively, of the polymer films supported on rough surfaces with different film thickness h_g. Shown in (c) and (d) are the analogous figures for rough and smooth surfaces for one film thickness $h_g = 15$. Near the free surface (large z), T_g decreases for both surfaces. Near the substrate (small z), T_g increases for film supported on a rough surface, but decreases for a smooth surface.

Chapter 6

String-like Cooperative Motion and Adam-Gibbs Theory

From the discussion in Chapters 4 and 5, there are a variety of factors that can alter the dynamics of thin polymer films, including film thickness, roughness, the polymer-boundary thermodynamic interaction and the stiffness of the boundary. Impurities introduced from the film casting process and possible heterogeneity in the substrate interfacial chemistry due to, e.g., substrate oxidation, are also known to be relevant [27]. These effects are clearly all significant and the observed changes of the film dynamics indeed involve the convoluted effect of all these relevant variables. Clearly, we need some organizing principle that could be used to reliably understand all these factors influencing film dynamics, which could be used conceptually to guide the development of polymer films with rationally engineered properties.

In Chapter 5 and in our previous studies [39], we have shown the limitations of using density or 'free volume' as an indicator of dynamical changes. The more suitable perspective on the dynamics of glassy materials put emphasis on the

importance of collective molecular motion in relation to understanding rates of structural relaxation. In this chapter, we explore this particular perspective to obtain a unified understanding of the diverse dynamical changes that we observe in polymer films subjected to various combinations of surface roughness, stiffness, and boundary interaction. This exercise will serve as a further test of the predictive power of the entropy theory of glass-formation.

6.1 Adam-Gibbs Theory

From a theoretical perspective, the arguments by Adam-Gibbs (AG) [47] provide a framework for understanding how the scale of cooperative motion relates to the time scale of structural relaxation. This was described qualitatively in Chapter 1. More specifically, according to the AG theory, the activation Gibbs energy is extensive in the size of CRR, so τ may now be written as

$$\tau(T) = \tau_0 \exp\left[\frac{z^* \Delta G}{k_{\mathrm{B}} T}\right], \tag{6.1}$$

where τ_0 is the high temperature limit of relaxation time, z^* is the number of particles involved in a cooperatively rearranging region (CRR), k_{B} is the Boltzmann factor, T is the temperature of the system, and ΔG is the activation free energy at high temperature. We note that at high temperature the particle motion should be independent of any cooperative behavior. This requires that z^* equals a constant at high temperature limit (AG originally assumed that $z^* \simeq 1$ at high temperatures, corresponding to completely uncooperative motion, but a constant value of z^* is all that is required to recover Arrhenius dynamics at high T).

Recent simulations have shown that despite the rather heuristic nature of the original arguments by AG, equation (6.1) with z^*, which is identified specifically

with the average extent of cooperative string-like particle exchange motion, provides a good description of the temperature dependence of the structural relaxation time in polymer melt simulations, even under the case when nanoparticles have been added to tune the fragility over a wide range [39, 60, 61]. In this chapter, we, for the first time, test the predictive capacity of the AG relation prescribed by equation (6.1) for the case of ultra-thin supported polymer films. Riggleman et al. [27] have previously evidenced that the scale of collective motion becomes diminished in free-standing film simulations based on a similar coarse-grained model to the present paper. According to Ref. [27], the fragility of polymer film tends to become reduced for specific boundary conditions and the film thicknesses considered in our study, in qualitative accordance with the expectations from equation (6.1). We therefore perform a quantitative test of equation (6.1).

As a first step, we consider the activation free energy ΔG. The activation free energy ΔG from even the simple Eyring transition state theory [72] contains both enthalpic ΔH and entropic ΔS terms, namely $\Delta G = \Delta H - T\Delta S$, although the entropic term has often been neglected from consideration. However, in recent work on polymer nanocomposites [61], this term was found to be important. We, therefore, retain the entropic term in the present analysis; as we shall see, this term apparently plays a significant role in understanding confinement effects in thin polymer films. In fact, Truskett and coworkers [80] take the entropy term to be the *primary* factor in the dynamics of dense fluids, so far as to neglect the enthalpic term in ΔG based on the assumption that the repulsive particle interactions predominate the inter-particle interactions. This seems reasonable at a first glance, but the common observation of Arrhenius temperature dependence of transport properties and reactions in the condensed phase clearly shows that the enthalpic contributions to the free energy barrier of transport can as well be relevant [60, 61]. Indeed, as a matter of fact keeping both the entropic and

enthalpic terms will turn out to be crucial in our analysis. This is so, because these free energy variables vary with film boundary conditions and film thickness. Appendix 9.1 discusses these variables and their expected variation in thin films.

AG are vague about the specific geometrical form and polydispersity of the CRR, and offered no viable computational algorithm for finding these structures [47]. However, recent computational studies [55, 60, 61, 81] have identified cooperative particle motion in the form of string-like units that grow in proportion to the activation free energy on cooling. The mean mass (length) L of these 'strings' has been found to give us a quantitive estimation of z^* in the AG theory, so this string model together with the available quantitative estimation of z^* goes beyond the original heuristic reasoning of AG. These dynamic polymeric structures have an exponential size distribution and statistical geometry of branched polymers [55], and recent work has shown the string properties can be quantitatively described by an equilibrium polymerization theory [81]. The analysis of the dynamics of our thin polymer films is then based on the string model of structural relaxation, in which τ is described by the AG inspired relation

$$\tau(T) = \tau_\infty \exp\left[\frac{L(T)}{T}(\Delta H - T\Delta S)\right], \tag{6.2}$$

where ΔH and ΔS are the familiar temperature independent activation energy parameters of transition state theory [72]. The applicability of this relation to all of the different polymer film conditions described provides a rather stringent test of this view on glass formation because of the wide range of fragility variations these films exhibit. It is not clear *a priori* whether such a model should apply effectively to such a generally inhomogeneous material. Previous success in applying equation (6.2) to polymer nanocomposites with the highly variability in fragility [61] suggests that the model might well apply, since nanocomposites are

also rather structurally inhomogeneous. One issue that must be confronted when treating thin films is that the energetic parameters ΔH and ΔS should change from their bulk values in films or, for instance, when additives such as nanoparticles are added to the polymer fluid. This is an important effect even without any consideration of collective effects on the relaxation dynamics We next compare our simulation data to this relation and check the physical sensibility of the fitted values of the energetic parameters.

6.2 Scale of Cooperative Dynamics L

As the first step toward testing the relationship between the scale of cooperative motions in polymer films and relaxation, we must evaluate the string size $L(T)$, following methods described in the previous works [82, 83]. Specifically, we select a set of most mobile particles as the top 6.5% of the particles with greatest displacement over time t. The details of identifying these strings and the T-dependence of L over time t are discussed in Section 3.2.5. In this section, we focus on how L changes with respect to boundary effects.

Figures 6.1 (a) and (b) compares the T dependence of L of films with distinct thicknesses supported on a rough or a smooth substrate. For a given film thickness, L is larger and grows faster for the film supported on a rough surface, which is qualitatively consistent with the T dependence of relaxation time τ [see figure 4.1 (a) and (b)], characterized by the changes of fragility [see figure 4.1(d)]. Similarly, the variation of $L(T)$ with interfacial interaction strength ϵ_{wm} or substrate rigidity k, shown in figs. 6.1 (c) and (d), also qualitatively captures the T dependence of relaxation time [see figures 4.2 (b) and (d)]. This qualitative similarity suggests that we can predict changes in fragility from the variation of $L(T)$ as found in previous works [27, 60, 61].

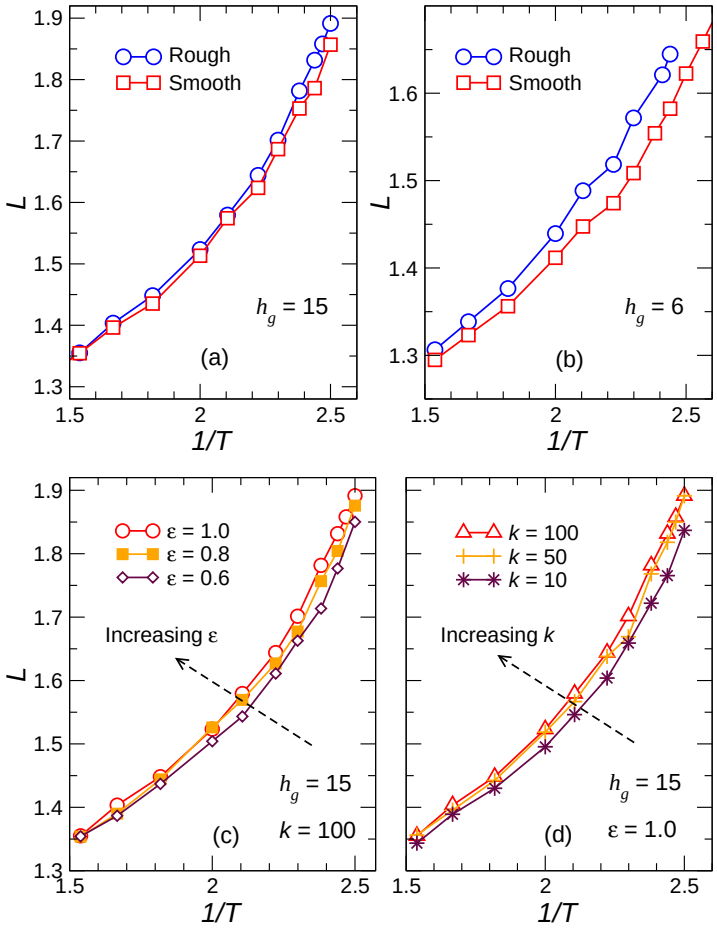

Figure 6.1: Average string length L as a function of $1/T$. Shown in (a) and (b) are the dependence of L on T for different film thickness $h_g = 15$ for (a) and $h_g = 6$ for (b). Note that both (a) and (b) have two separate cases where films are introduced to either a rough (circles) or a smooth (squares) surfaces. The different T dependences of L for the different polymer-substrate interaction $\epsilon_{\rm wm}$ and for different substrate rigidity k are shown in (c) and (d), respectively. The variation of the T dependence of L captures the T behavior of structural relaxation time τ with varying the relevant parameters (see figure 4.1 and figure 4.2). This qualitative consistency shows the applicability of AG theory employing cooperative dynamics, characterized by L, in quantifying the T dependence of τ, characterized by fragility.

6.3 Analysis of Collective Motions as an Organizing Principle for Thin Films Dynamics

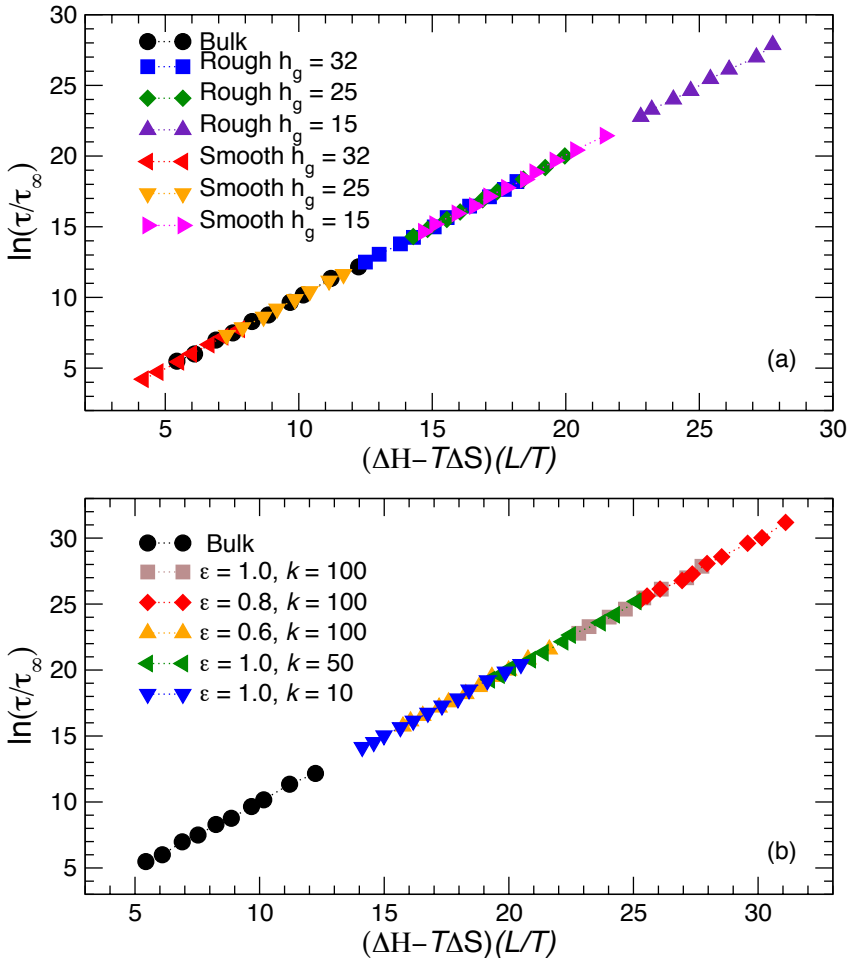

Figure 6.2: Linear collapse of structural relaxation time τ with the average strings size L for (a) various thicknesses and (b) various polymer-substrate interactions or surface rigidities. The data are scaled with parameters ΔH, ΔS and τ_∞ from the fitting AG relation equation (6.2).

Now that we have L for all conditions, we can test the applicability of the AG theory in equation (6.2) to quantify the dynamical changes with varying film thick-

ness, polymer-substrate interaction, or substrate rigidity. Figure 6.2 (a) shows the collapse of all data points in one universal line holds for all film thicknesses supported on a rough or a smooth substrate as well as a bulk system[1]. The qualitative collapse is amazing. In figure 6.2 (b), we show an equivalent plot of a representative film supported on a rough substrate, this time collapsing various interfacial interaction or substrate rigidity on to a single universal line. The form of the two collapse is identical between the figure panels, we only separate them for clarity. This remarkable result shows that we can make a generalization in characterizing all film dynamics, despite a wide range of dynamical changes due to film thickness, polymer-substrate interaction, or surface rigidity, by relating structural relaxation time with cooperative dynamics quantified by the average string length L. Therefore, we appear to have identified the proposed organizing principle to rational our thin film results. This result also supports the idea that the scale of cooperative motions is proportional to $\Delta G(T)$, showing that L is the molecular realization of CRR.

It is important to understand the significance and the physical meaning of the fit parameters in the AG relation. First, we consider the behavior of the prefactor, τ_∞. Treating this as a free parameter, we found that τ_∞ varies by several orders of magnitude, becoming as small as $O(10^{-7})$. Since τ_∞ can be interpreted as an inverse attempt frequency the existance of such small value at first seems unphysical. Accordingly, we now explore a physical understanding of this variation.

[1] τ_∞, ΔH and ΔS are obtained as fit parameters in equation (6.2)

6.4 Influence of Confinement on Chain Conformational Entropy

In this section we describe a framework for the variation of τ_∞. We propose that the changes in τ_∞ can be associated with changes in chain conformational entropy, which is controlled by the system size h (film thickness at any given temperature). When polymer chains become confined on a scale comparable to the chain radius of gyration R_g, the free energy of the polymer fluid changes in a way that is significant in magnitude and universal in general functional form. This effect is particularly significant for the chain conformational entropy since the number of chain configurations depends strongly on the spatial dimension. In particular, it is well known from chromatography applications [84] and modeling in the field of rubber elasticity [85] that confinement changes chain conformational entropy by a contribution that scales as a negative power of the confinement scale h,

$$\Delta F_c \sim -(R_g/h)^\alpha. \tag{6.3}$$

We are particularly interested in the scaling exponent α, which equals 1 for random walk chains under physical condition in which the chain monomers occupy space uniformly (reflecting boundary conditions). In particular, Dayantis and Sturm found that $\alpha = 1$ for Gaussian chains confined by with reflecting boundary (RB) conditions, or $\alpha = 2$ for absorbing boundary (AB) conditions [86]. They argue that confined chains should obey AB statistics ($\alpha = 2$) provided the confinement size $h \gg R_g$, and should obey RB statistics ($\alpha = 1$) when $h \sim 2R_g$. At intermediate h, one expects an intermediate behavior of α. This provides a physical way to comprehend the behavior of τ_∞.

Combining equation (6.2) and (6.3), we then obtain the extension of our bulk

expression for τ to describe relaxation in

$$\tau = \tau_\infty(\text{bulk}) \exp\left[-(aR_g/h)^\alpha \right] \exp\left[\frac{L(T)}{T} [\Delta H(h) - \Delta S(h)] \right] \tag{6.4}$$

where a and α are a constants that captures the thickness dependence of the relaxation prefactor τ_∞. Thus, while chain confinement has a limited effect on the localization of T_g [39], chain confinement should affect the rate of relaxation by influencing the basic energetic parameters of activated transport. In general, that parameter a is unspecified by our general scaling analysis can be expected to depend on boundary roughness and the polymer-surface interaction strength. The energetic parameters must also depend on chain length, but our simulations in the present work are limited to a constant chain length. In the limit of film thickness $h \to \infty$, we must recover by consistency the bulk AG relation,

$$\tau(T) = \tau_\infty(\text{bulk}) \exp\left[\frac{L(T)}{T} (\Delta H - T\Delta S) \right]. \tag{6.5}$$

For the case of a polymer melt, we expect $\alpha \sim 1$ as a reasonable model for uniform density polymer films and, based on our discussion above, we take this scaling relation to also apply to the activation free energy $\Delta S(h)$ of our thin polymer films as a function of film thickness, h. Similar reasoning applies to shifts of second-order phase transitions which can also be understood quantitatively from a shift in activation entropy of random walk and self-avoiding walk chains [87].

For our films, we must therefore consider the nature of interfacial interactions at each boundary. The behavior of the free surface is known to be very similar to that of a hard, impenetrable wall. We have previously shown that the smooth wall – even with attraction – shows the same interfacial changes. Thus, we would anticipate that the smooth substrate should obey RB statistics ($\alpha = 1$). For the rough substrate, the interfacial dynamics are changed opposite those of the smooth substrate. Thus, the rough surface might be expected to be more like

the AB statistics. However, the rough substrate is in competition with the free boundary, potentially resulting in some intermediate behavior ($1 < \alpha < 2$).

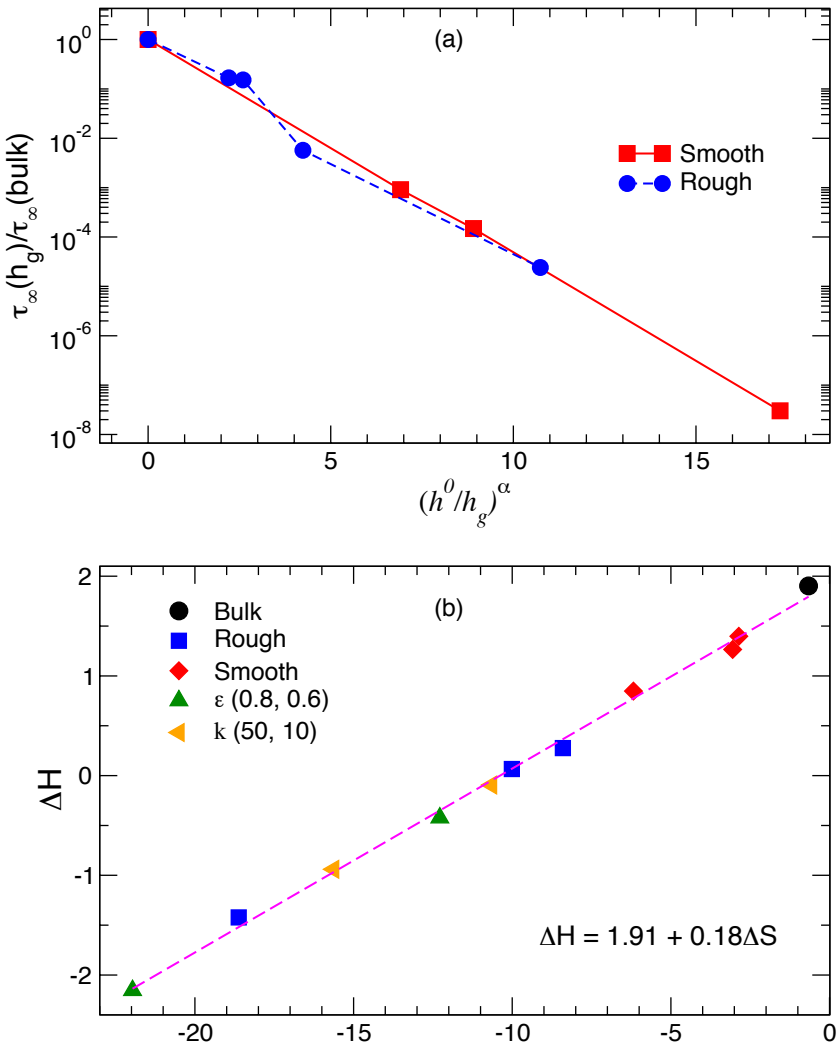

Figure 6.3: (a) The collapse of $\tau_\infty(h_g)$ as function of the inverse of h_g. The data are scaled with $\tau_\infty(bulk)$, $h^0 \equiv a \times R_g$, and α. a and α are obtained from fitting our data to equation (6.4). (b) Variation of ΔH and ΔS for different film thicknesses, surface roughness, interfacial interactions, and substrate rigidities. The slope defines compensation temperature $T_{\rm comp} = 0.18$.

For our films, R_g is relatively constant for all film thicknesses. We can also ne-

glect the T dependence of film thickness, since thickness does not vary significantly with T. We choose $h = h_g$ as the confinement scale and treat R_g as a constant value. With these considerations, we find $\alpha \sim 1$ for the smooth substrate and $\alpha \sim 1.3$ for the rough substrate. Figure 6.3 (a) shows how $\tau_\infty(h_g)$ normalized τ_∞ of the bulk varies as function of inverse of film thickness at T_g scaled by a and α [see equation (6.8)]. This suggests that the smooth substrate follows a boundary condition close a reflecting boundary condition where the density is very uniform, consistent with our expectation. The rough substrate has a best fit value $\alpha \sim 1.3$, consistent with an intermediate boundary condition between reflecting and absorbing boundary, an effect presumably associated with a physically non-uniform density near such boundaries. Note that, at the compensation temperature when $\Delta H - T\Delta S = 0$ (see below), the prefactor $\tau_\infty \propto \exp\left[-(aR_g/h)^\alpha\right]$ is entirely responsible for the variation of τ_∞ with film thickness, and can therefore be entirely attributed to the confinement effects.

6.5 Influence of Confinement on Activation Free Energy Parameters

Having established a framework to understand thickness dependence of τ_∞, we next examine variation of activation free energy parameter ΔH and ΔS in supported polymer films. We obtained ΔH and ΔS from fitting our data to equation (6.2). Figure 6.3 (b) shows the variation of ΔH and ΔS for various film thicknesses, substrate structure (smooth or rough), interfacial energy, and surface rigidity. In general ΔH and ΔS decreases with decreasing film thickness.Interestingly, we find all data collapse in a single line. Using a simple linear function, we can

write ΔH as

$$\Delta H(h_g, \epsilon, k) = \Delta S(h_g, \epsilon, k) T_{\rm comp} + \Delta H_0. \tag{6.6}$$

The slope of this linear equation, which defined as compensation temperature $T_{\rm comp} \sim 0.18$, is very close to the previously identified Kauzman temperature ($T_{\rm k} = 0.2$ for the bulk material) [55], the temperature at which the configurational entropy $S_{\rm conf}$ formally extrapolates to 0, and structural relaxation time extrapolates to infinity. The proportionality between ΔH and ΔS having a slope ~ 0.2 also appears in simulation of polymer nanocomposites based on the same polymer model [81].

Now consider the compensation temperature $T = T_{\rm comp}$, where ΔG reduces to the relation

$$\Delta G = \Delta H(h_g, \epsilon, k) - \Delta S(h_g, \epsilon, k) T_{\rm comp} = \Delta H_0. \tag{6.7}$$

At this temperature, the activation free energy ΔG does not depend on the geometry (confinement size) or other relevant factors related to the boundary conditions. Although ΔG is universal at $T_{\rm comp}$, the relaxation time τ is not universal because τ depends on chain conformational entropy which has thickness dependence,

$$\tau(T_{\rm comp}) = \tau_\infty({\rm bulk}) \exp\left[-(aR_g/h)^\alpha \right] \exp\left[\frac{L(T_{\rm comp})}{T_{\rm comp}} (\Delta H_0) \right]. \tag{6.8}$$

This result shows that the non-universal value of τ at $T_{\rm comp}$ is the consequences of the changes in configurational entropy of the chains due to their confinements. Our findings show the applicability of cooperative dynamics in determining structural relaxation time in terms of AG theory. We also show that the confinement effects may greatly affect the total configurational entropy of the whole film which leads to the variation of τ of the films even at $T_{\rm comp}$ where ΔG is independent of film thickness or other relevant factors related to the boundary conditions. More detailed discussions on variation of ΔG and ΔS can be found in Appendix 9.2.

6.6 Summary

We have systematically explored obvious potential factors to understanding the dynamics of thin supported polymer films, film thickness, surface roughness, polymer-surface interaction strength, and the rigidity of the supporting substrate. All these factors were found to be highly relevant to the dynamics of our simulated polymer films and their coupling makes an understanding of changes in polymer film dynamics in thin films rather complicated. Simple free volume ideas are simply not adequate to understanding the significant variations in film dynamics that we observe so that static scattering observations should be of little value in predicting dynamical changes in thin polymer films. A high level of control on the boundary structure and interaction are evidently necessary to make polymer films with reproducible properties. Moreover, prediction of film properties based on computation will require the specification of many factors related to the film boundary conditions.

Despite this wide range of changes of film dynamics with boundary conditions and supported film thickness, we find that we obtain a remarkably general characterization of the changes in all film dynamics using the string model of structural relaxation. We thus have an effective unifying perspective of the changing dynamics of supported polymer films based on how the collective motion is perturbed in the film state The problem remains, however, of determining the extent of string-like collective motion in real materials. Preliminary recent work suggests that noise measurements might be effective for estimating average string length L [88]. Thus, in the next chapter we address how the extent of collective motion can be effectively estimated from direct measurement.

Chapter 7

The Relation between Cooperative Motion and the Scale of Interfacial Mobility

For bulk glass formers, both the Adam-Gibbs (AG) [47] and the random first-order transition (RFOT) [48] theories both have provided convincing evidences that there is an intrinsic scale that controls the variation of relaxation time approaching the glass transition temperature T_g. From previous chapter and our recent works [55, 60, 61], we have found that this intrinsic scale can be related to the characteristic scale of the string-like cooperative motion, providing a molecular realization of the abstract cooperatively rearranging regions (CRR) invoked by AG and RFOT. However, direct experimental observations of this string-like cooperative motion in molecular glass-forming liquids remains a central challenge.

In Chapter 5, we observe that near interfacial regions (substrate or free-surface) dynamics are different from the that of the bulk. Therefore, it is possible define a length scale by examining the depth of perturbations caused interfaces, and

such of scales can also be measured experimentally [22, 34, 46]. It is natural to ask to what degree this scale relates to the scale of CRR. Stephenson and Wolynes [62] have argued, based on the RFOT theory and scaling arguments, that the interfacial mobility length of films should scale inversely to the configurational entropy of the films. Combining this result with the results showing that the string length scales inversely to the configurational entropy [55], we then might expect the interfacial mobility length should scale in proportion to the string length, and thus describe the temperature T dependence of relaxation. Very recently, Simmons and coworkers [63] indeed found that the interfacial mobility scale grows in proportion to the apparent activation energy for relaxation from molecular dynamics simulations of polymer films, suggesting that this scale provides an estimate of the collective motion scale from the AG model. Our previous study [55] also showed that RFOT is consistent with our observations of string-like collective motion if the size of the entropic droplets of this model is equated to the radius of gyration of the strings, further motivating the investigation of the potential direct relation between the scale of string-like collective motion and the interfacial mobility scale.

In this chapter, we address how the the scale ξ of interfacial dynamics at the polymer-air interface of polymer films supported on rough or smooth surfaces with variable substrate interaction strength can be related to the scale of collective motion L in films. This offers a possible route to experimentally probe the scale of cooperative relaxation.

7.1 Interfacial Mobility Scales ξ

To quantify interfacial dynamics and the corresponding interfacial length scale, we resolve the dynamics locally. We first contrast the local dynamics as a function

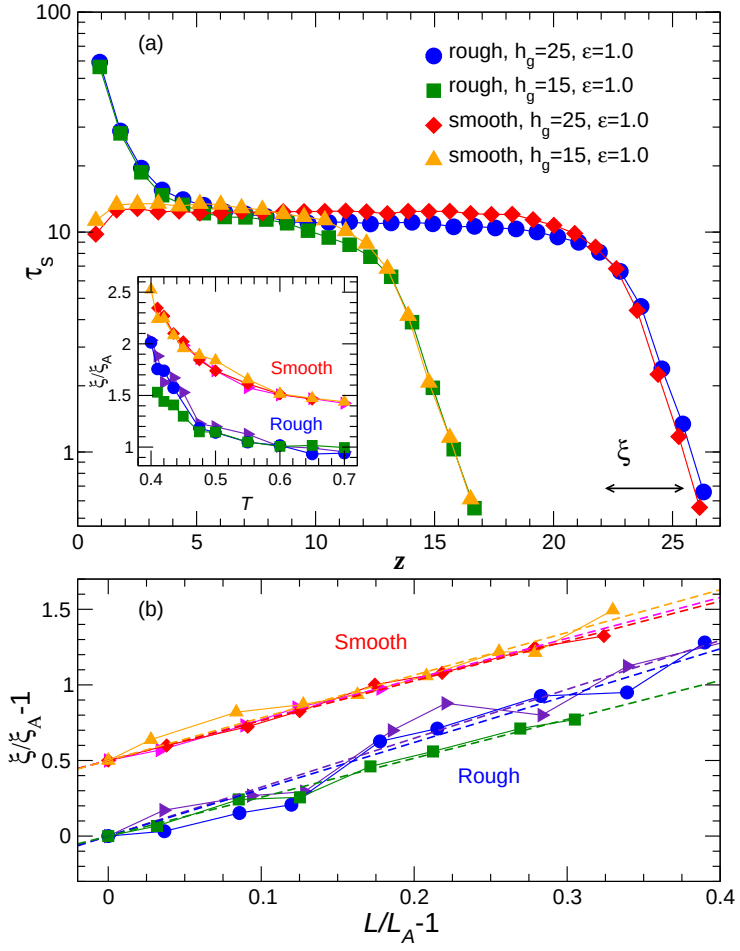

Figure 7.1: (a) The local relaxation time τ_s as a function of distance z from the substrate for films supported on rough or smooth surfaces. The inset shows the resulting free surface mobile layer scale, ξ, for films supported on a rough or smooth substrate as function of temperature T; ξ is normalized by ξ_A, where ξ_A is the value of ξ at the Arrhenius temperature T_A. We also show ξ data for thickness $h_g = 32$ (triangle right) in the inset. The values of ξ for the smooth surface are shifted by 0.5 for clarity. (b) $\xi/\xi_A - 1$ for films supported on rough or smooth surfaces as a function of $L/L_A - 1$, showing proportionality between these quantities. Note that L_A is the value of L at T_A. The normalized $\xi/\xi_A - 1$ of films on a smooth surface is shifted by 0.5 for clarity of the figure.

of distance z from the substrate boundary of the rough or smooth surfaces with $\epsilon_{\rm wm} = 1$. To do so, we evaluate the self-part of the dynamical density correlation function equation (3.9), and condition it by the the distance z from the substrate in intervals $\delta z = 0.875$, as we did in Chapter 5. From this analysis, we obtain the distance dependence of self relaxation time $\tau_{\rm s}(z)$. Figure 7.1 (a) shows that, starting from the free interface (large z), to the film center, $\tau_{\rm s}(z)$ has nearly the same z dependence for rough or smooth surfaces; $\tau_{\rm s}(z)$ differs for rough and smooth substrate at distances close to the surface (z=0). Specifically, $\tau_{\rm s}$ increases close to the rough surface, but decreases near the smooth surface. Due to the smoothness of the perfectly flat substrate, monomers can "slide" along the substrate resulting enhancements near the smooth surface, so that relaxation parallel to the substrate is more rapid than relaxation perpendicular to the substrate (see Refs. [39, 79]). This anisotropy disappears for the rough surface we study.

We next quantify the dynamical length scale ξ of the free-interface (mobile-layer scale) based on local relaxation time $\tau_{\rm s}$ near the free surface, as we did in our previous work (see Ref. [39] for a detailed description). A similar choice, as well as other choices, was examined by Simmons and coworkers [63]. We define ξ as the length where $\tau_{\rm s}$ deviates by some percentage from the nearly constant value at the film center. A natural question is whether our findings for the interfacial scale ξ have a strong sensitivity to the choice for the allowed deviation of $\tau_{\rm s}(z)$ from its value at the film center. Figure 7.2 tests the robustness of our definition of ξ for several cutoff choices. It is apparent that the choice of the cutoff does not change our qualitative findings, provided that the choice is large enough that fluctuations in $\tau_{\rm s}(z)$ do play a role ($\gtrsim 15\%$ for these data) but small enough to be meaningful ($\lesssim 50\%$). An advantage of this definition is that it depends both on the behavior near the interface, as well as near the mean value of the film center. We find below that both contributions are important for our results. We limit

our analysis to films in which the interfacial scale is no larger than half of the film thickness, since this is a limiting value [39]. In this analysis, we specifically define ξ as the length where τ_s deviates by 30 % from the nearly constant value at the film center. For reference, we note that the values of $L(T_A)$ and $\xi(T_A)$ (using the cutoff choice 30 %) are relatively constant for all systems; specifically, $L_A \approx 1.41$ and $\xi_A \approx 3.6$.

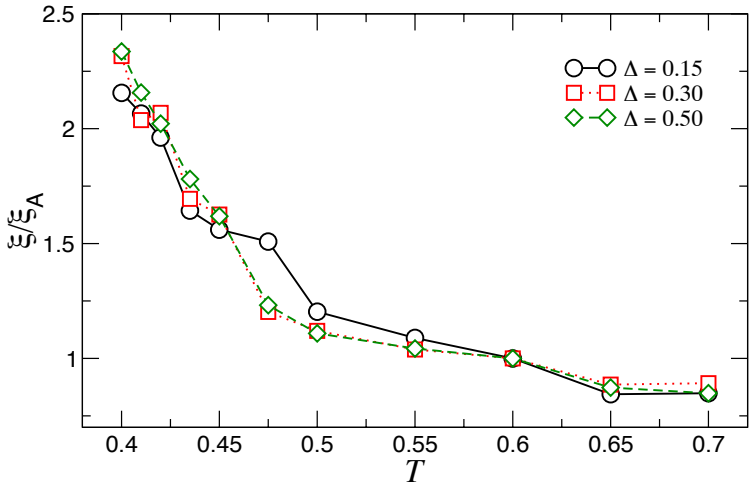

Figure 7.2: Interfacial mobility scale ξ as a function of temperature T. Interfacial mobility scale ξ defined by the length where τ_s deviates by 15 %, 30 %, or 50 % from the nearly constant value at the film center. The T dependence for all choices is nearly identical. The values of ξ are normalized by their values at T_A to remove the trivial effect of changing the cutoff percentage.

7.2 Relationship between ξ and L

The inset of figure 7.1 (a) shows the growth of ξ with decreasing T for four representative films supported on a rough or a smooth surface. ξ is normalized by its value at the onset temperature T_A for "slow" dynamics [1]. This typical growth

[1] In glass-forming systems, the appearance of non-Arrhenius T dependence and cooperative motion only occurs below an 'onset' temperature T_A, which for our system is approximately 0.6.

of dynamical length scales has been observed in other computational studies [38, 39, 63, 77]. It is also important to recognize that this interfacial mobility scale is *independent* from the scale of interfacial density changes [39].

We next consider the possible relation of the interfacial scale to a dynamical heterogeneity scale. As discussed in Chapter 6, glass-formers are dynamically heterogenous, evidenced by spatial correlation in mobility. In particular, computer simulations [27, 47, 49–55] and colloidal experiments [56–59] have shown the existance of cluster formation of the most mobile particles, and these most mobile particles tend to move coolinearly in string-like fashion. We, therefore, aim to test whether the interfacial scale might be reflective of this scale of cooperative motion. Accordingly, we evaluate average size of string-like cooperative motion, $L(T)$. We evaluate $L(T)$ following the methods described in Chapter 3 (see Ref. [55] for more details). Figure 7.1(b) shows that L and ξ grow proportionally, relative to their values ξ_A and L_A at the the onset temperature $T_{\rm A}$,

$$\big[L/L_{\rm A} - 1\big] = A\big[\xi/\xi_{\rm A} - 1\big]. \tag{7.1}$$

The proportionality constant A fluctuates with no apparent trend around a mean $A = 0.32$. Given that L varies inversely proportional to the configurational entropy $S_{\rm conf}$ [55], ξ should also vary inversely proportional to $S_{\rm conf}$ (with the factors of $\xi_{\rm A}$ and $L_{\rm A}$ included) broadly consistent with the prediction by Stephenson and Wolynes [62]. This provides our first indication that the interfacial scale might indeed reflect a fundamental heterogeneity scale.

To further test the robustness of the possible relation between interfacial and heterogeneity scales, we extend our analysis to consider variations in surface-polymer interaction strength $\epsilon_{\rm wm}$ and surface rigidity k. Analogous to $\tau_{\rm s}(z)$ shown for smooth and rough surfaces, figure 7.3(a), shows $\tau_{\rm s}(z)$ increases near the substrate as we increase $\epsilon_{\rm wm}$, since stronger interfacial interactions enhance the trap-

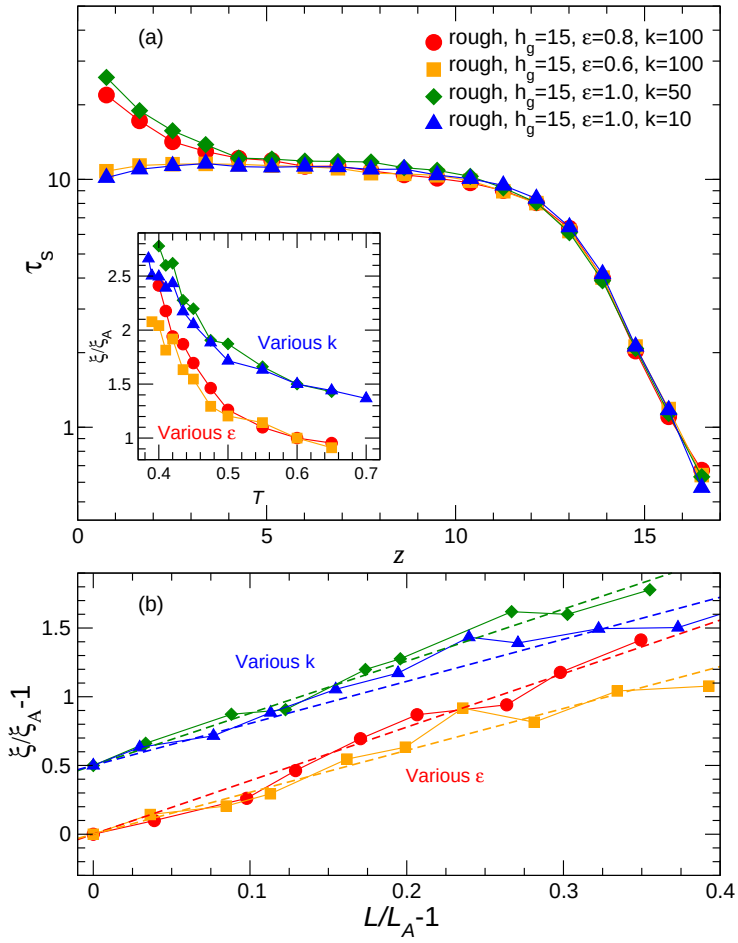

Figure 7.3: (a) The local relaxation time $\tau_{\rm s}$ as function of distance z from the substrate for various interfacial energies $\epsilon_{\rm wm}$ and surface rigidities k. The inset shows mobile layer scales ξ for films supported on a rough surface with various ϵ and k as function of temperature T, where ξ is normalized by its value at $T_{\rm A}$. The values of ξ for substrate with different k are shifted by 0.5 for clarity. (b) $\xi/\xi_{\rm A}-1$ for films supported on rough surface as function of $L/L_{\rm A}-1$, indicating their apparent proportionality. The normalized $\xi/\xi_{\rm A}-1$ values for substrates with different k are shifted by 0.5 for clarity of the figure.

ping of monomers near the attractive substrate. Likewise, decreasing wall rigidity k allows monomers to move more freely, since the wall atoms are less strongly

localized.

From these data we obtain ξ just as done for the previous case where we extract ξ from films supported on smooth or rough surfaces. The dependence of ξ on $\epsilon_{\rm wm}$ and k is not obvious, since $\tau_{\rm s}(z)$ appears both nearly identical near the free surface for various $\epsilon_{\rm wm}$ and k. However, the behavior near the interface and *at the center* play a role in determining the variation of ξ. Since the values for $\tau_{\rm s}(z)$ near the film center differ for different $\epsilon_{\rm wm}$ and k, we find a modest but non-trivial difference in ξ as the suface properties change. Figure 7.3(a) inset shows that ξ increases on cooling [similar to figure 7.1 (a) inset]. Moreover, figure 7.3(b) confirms the apparent proportional variation between in $\xi/\xi_{\rm A} - 1$ and $L/L_{\rm A} - 1$, consistent with our findings in figure 7.1(b). This supports the hypothesis that ξ and L are related.

7.3 Determining Relaxation Using Interfacial Mobility Scale ξ in terms of AG theory

To demonstrate the physical importance of such a relation, consider that according to the AG theory, the activation energy is extensive in the size of CRR, so that τ (for the entire film) can be related with the average string size L by

$$\tau(T) = \tau_\infty \exp\left[\frac{L(T)}{L_A}\frac{\Delta\mu}{k_{\rm B}T}\right], \tag{7.2}$$

where $\Delta\mu$ is the limiting activation free energy at elevated temperatures where τ has Arrhenius dependence. $\Delta\mu$ contains both enthalpic ΔH and entropic ΔS terms, so that $\Delta\mu = \Delta H - T\Delta S$ (see Chapter 6 for detailed discussions). In equation (7.2), we normalize $L(T)$ by $L_{\rm A}$, so that the ratio approaches 1 as $T \to T_{\rm A}$ [2].

[2]Note that normalization by L_A in the AG relation [equation. (7.2)] is not strictly needed (as we previously did in Chapter 6), since it simple redefines the values of ΔH and ΔS; however, it

Figure 7.4 (a) confirms the applicability of the string size to quantify dynamical changes in polymer films *under all conditions examined*, including variable film thickness, surface roughness, and polymer-substrate interaction, as we had shown in Chapter 6. While such a relation has been shown in bulk and polymer composite systems [55, 60, 61], here we demonstrate the applicability to polymer films for a wide range of surface conditions and film thicknesses. The remarkable degree of data collapse in figure 7.4 (a) provides strong evidence supporting the identification of the strings with the abstract CRR of AG.

Since there is no readily accessible experimental measurement of string-like cooperative motions, and since we found an apparent proportionality between L and the interfacial scale ξ, we consider if ξ can be used as a substitute for L. Combining equations (7.1) and (6.1) suggests an AG-like relation between τ and ξ,

$$\tau = \tau_\infty \exp\left[\frac{(1-A)\Delta\mu}{k_\mathrm{B}T}\right] \exp\left[\frac{\xi(T)}{\xi_A}\frac{A\Delta\mu}{k_\mathrm{B}T}\right]. \tag{7.3}$$

Our data indicate that the T dependence of the leading term $\exp[(1-A)\Delta\mu/k_\mathrm{B}T]$ is weak in comparison to the term involving ξ, both because $1-A$ is relatively small and since ξ grows on cooling. Consequently, if one approximates the first exponential term as constant, the expression simplifies to

$$\tau \approx \tau_\xi \exp\left[\frac{\xi(T)}{\xi_A}\frac{A\Delta\mu}{k_\mathrm{B}T}\right]. \tag{7.4}$$

More generally, without approximation, $\tau_\xi = \tau_\infty \exp[(1-A)\Delta\mu/k_\mathrm{B}T]$. The approximation that τ_ξ is constant is important for possible experimental application, since L (and hence A) is not easily measured. Using this approximation, we find that ξ works nearly as well as L to describe $\tau(T)$ using the same ΔH and ΔS values already determined from the relation of τ with L. In other words, we do

is convenient to include L_A when using equation (7.1) to recast the AG relation in terms of ξ.

not allow these parameters to be refit. This parameterization results in a collapse of all data shown in figure 7.4 (b).

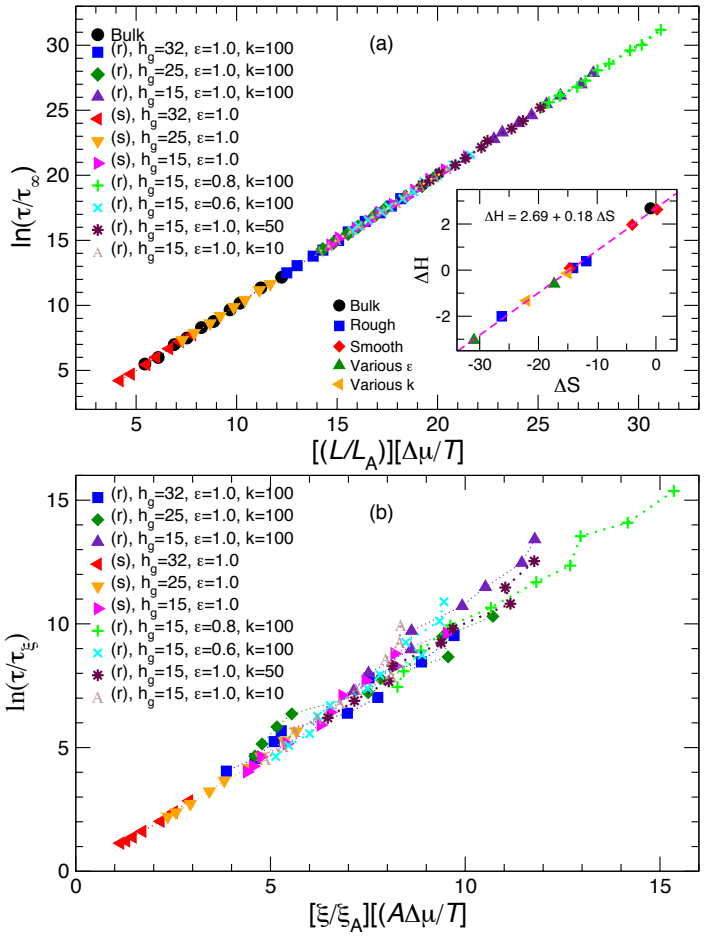

Figure 7.4: Test of the AG relation using string size L and interfacial scale ξ. (a) Collapse of $\ln(\tau/\tau_\infty)$ vs $[L/L_\mathrm{A}][\Delta\mu/T]$ for all systems. (b) Collapse of $\ln(\tau/\tau_\xi)$ vs. $[\xi/\xi_\mathrm{A}][(A\Delta\mu)/T]$ for all systems. Inset (a) shows the proportionality between ΔH vs ΔS for all systems with an entropy-enthalpy compensation temperature slope $T_\mathrm{comp} \approx 0.2$.

The data collapse shown in figure 7.4 depends on the parameters ΔH and ΔS. Thus, it is natural to consider how these quantities vary. Curiously, the inset of figure 7.4 (a) shows a linear dependence of between ΔH and ΔS, the slope of

which defines an entropy-enthalpy 'compensation temperature' $T_{\text{comp}} \approx 0.2$. The origin of this particular value poses an interesting question for future study.

7.4 Summary

The high interfacial mobility of both glassy and crystalline materials is a problem of profound importance for both a fundamental understanding of glass-formation and technological applications. The physical picture, derived from both the classical AG theory and the more recent RFOT theory, suggests that the strong temperature dependence of relaxation times in glass-forming liquids derives from the growing extent of the collective motion on cooling, and our findings support interpreting the string size as this scale of collective motion. We further address how the dynamical interfacial layer might be related to collective molecular motion.

In particular, Stephen and Wolynes [62] argued that the interfacial mobility scale is inversely proportional to the configurational entropy S_{conf} [55], which implies that the interfacial scale ξ of glass-forming liquids should scale in direct proportionality to L. We have validated a very similar relationship in our simulations. Significantly, we have shown the validity the relation of L to τ and to ξ for a variety of surface energies and for a range of boundary stiffnesses on model rough and smooth surfaces, supporting the generality.

Simmons and coworkers [63] recently observed a relation between τ and ξ mathematically equivalent to equation (7.4) where, in effect, the constants τ_ξ and A in the prefactor and exponent were freely adjusted to fit their relaxation time data for a similar coarse grained polymer model. They did not quantify collective motion in their films so their findings were only suggestive of a relation between ξ and the CRR scale.

Our findings help to advance our understanding of collective motion in glassy materials, and the impact of these collective motions on the interfacial mobility of glassy materials. At the same time, our results suggest a practical metrology for estimating changes in the scale of collective motion in glassy materials that might be used in the design of advanced materials.

An important aspect of our work is that it opens a possible route to indirectly access the cooperativity scale in experiments. Similarly, the scale of collective particle motion was found to relate to the 'colored noise' exponent describing particle displacement fluctuations in the glassy interfacial zone of Ni nanoparticles [88]; however, this suggested relation has not been confirmed in ordinary glass-forming liquid. Tanaka and coworkers [89] have also found a relationship between the interfacial mobility scale as we have defined it and a correlation length associated with clusters having high local order and a class of particles that is highly immobile. The observations of the present work suggests that there might be complementarity between these different types of clusters of extreme mobility, and future work should explore this relationship.

Chapter 8

Conclusion

In the first part of this thesis, we have systematically explored potential factors that may affect dynamics of polymer films. Evidently, we find that glass transition temperature and fragility of our simulated supported polymer films are sensitive to film thickness, surface roughness, polymer-substrate interaction strength, and surface rigidity. To understand the observed changes in overall dynamics, we examine both dynamic and structural properties of polymer films locally. Free volume layer (FVL) idea provides a simple picture to rationalize changes in dynamics of polymer films: enhanced dynamics are associated with available space in that region (low density), while slow dynamics are associated with a dense environment. Our analysis on local relaxation time (dynamics) and density shows the limitation of this simple free volume layer idea in explaining the significant variations in dynamics of polymer films. For instance, we find a great difference in relaxation time at smooth and rough surfaces, but no difference observed in density analysis. Our findings suggest that (i) producing polymer films at nanoscale requires a high level of control on interaction and boundary structure and (ii) observed changes in dynamics are not necessarily connected to observed changes

in structural properties (e.g. density).

Despite wide property changes in film dynamics –due to variation in film thickness, surface roughness, polymer-substrate interaction, and surface rigidity– we obtain a unified framework to generalize all film dynamics using the string model of structural relaxation. We thus have an effective way to describe dynamics of supported polymer films based on how we perturb collective motions in films. However, the experimental measurements of string-like cooperative motion in real material remains a challenge. Motivated by this, we further address how the interfacial mobility scale –which can be accessed in experiments– might be related to the scale of collective molecular motions.

We also study the confinement effects on the activation free energy parameters from equation (6.2). We find a scaling relation to describe the changes in confinement free energy [see equation (6.3)] in respect to changes in film thickness based on the assumption that chain conformational entropy should change as the polymer is confined to a scale comparable to the radius gyration of the polymer. Understanding this scaling relation is important for producing advanced nanoscale materials, because we find that the scaling depends on the chain length, surface roughness, and polymer-substrate interaction. As we only studied one chain length, future study should address whether this scaling still holds for different chain length or for polymers confined in other geometry, such as nanotubes and nano-spheres.

In particular, Ref. [55] performed exact calculations on configurational entropy S_{conf} of a bulk polymer melt and showed that the size of string-like cooperative motion scales inversely proportional to the configurational entropy. To our knowledge, calculations on configurational entropy of confined polymeric material has not been done either in computer simulations or in experiments. Since we are able to generalize all film dynamics based on analysis of strings-like cooperative

motions, we expect that configurational entropy of polymer films may have a direct link to the significant changes in glass-transition temperature and fragility of polymer films.

Many recent experimental studies of glass-forming polymer films are now able to examine the variation of dynamics in polymer films [22, 34, 46] with a high precision and they found a relatively high-mobility interfacial layer near the polymer-air interface. In principle, we can extract a scale from the variation of mobility at these interfaces. We, therefore, test the possibility of relating interfacial mobility thickness ξ to the scale of collective motion within the film. Combining the arguments that the interfacial mobility scale ξ is inversely proportional to the configurational entropy S_{conf} [62] with arguments that S_{conf} is inversely proportional to the size of string-like cooperative motion L [55], we hypothesize that ξ can be directly related to L. We have validated such a relationship in our simulations. Significantly, we have shown the validity of the relation of L to τ and to ξ in describing all film dynamics, supporting the generality.

Through these findings, we now have a better understanding on how the collective behavior relates to the interfacial mobility gradient in glassy materials. This helps to further our understanding of glass formation, and is not limited to confined systems, where interfacial mobility scale may not be well defined. Tanaka and coworkers [89] found a correlation length from a class of highly immobile particles and clusters having high local order, and this correlation length is found to have connections with the interfacial mobility scale. This observation combined with our result suggests the possibility of relating clusters with high mobility to that are highly immobile. Future work should explore such a relationship.

In summary, we have explored how dynamics of polymer films can be greatly altered by relevant factors, such as film thickness, boundary structure, and surface-polymer interaction. All of these dynamical variations can be understood in a

unified framework using the scale of collective motions in films; however, this dynamical scale is not accessible in experiments. We then find an interfacial scale –which is experimentally accessible– that can be related to the scale of collective motion, and thus we are able to characterize all film dynamics using this interfacial scale. Having established a precise functional form relating the interfacial mobility scale and the scale of collective motion, we provide a practical importance for estimating changes in the scale of string-like cooperative motion that might have future applications for high-tech devices.

Chapter 9

Appendix

9.1 Effects of Film Thickness on Transition State Energetic Parameters of Supported Polymer Films

We take transition state theory as our starting point for describing relaxation in our thin polymer films in the absence of collective motion. This description is then extended to include the effect of collective motion, providing a means of general scheme for reducing our supported film relaxation data.

Within transition state theory [72, 90, 91], the diffusion coefficient, structural relaxation time and shear viscosity can all be described by an Arrhenius temperature dependence. For specificity, we consider the case of the structural relaxation time τ,

$$\tau = \tau_\infty \exp\left[\frac{\Delta G}{k_\mathrm{B}T}\right] \quad \Delta G = \Delta H - T\Delta S, \tag{9.1}$$

where and τ_∞ is a pre-factor related to local vibrational motions in simple fluids having a typical order of magnitude of 10^{-13}s , and the activation free energy ΔG

associated with the molecular displacing unit, corresponding to a polymer statistical segment in the case of polymers [92, 93], has separate energetic contributions ΔH and ΔS related to the strength of the intermolecular cohesive interaction strength and an entropic contribution related to coordinated motions required to surmount energy barriers in condensed materials [94–97].

While the direct link between the 'activation energy ΔH and the heat of vaporization and other measures of the intermolecular cohesive interaction has long been recognized both theoretically (at least within simplified fluid models) and experimentally [98–100], the variation of the entropy of activation ΔS with molecular parameters is much less understood. In simulations of molecules having simple Lennard-Jones interactions, it has been established that ΔH scales in proportion to the interaction parameter ϵ [101–103] and ΔS is often found to be roughly constant, at least at elevated temperatures where glassy dynamics does not prevail. The situation is similar for many small liquids and this has led to a preoccupation with the ubiquitous activation energy parameter ΔH. However, molecules with many internal degrees of freedom such as polymers can exhibit a considerable experimental variation in ΔS [94]. In particular, a survey by Bondi [94] revealed that ΔS could vary over a 100 entropy units $\Delta S/k_B$ and even can change sign so that ΔS cannot possibly be ignored.

A basic problem in developing a theoretical model of relaxation in polymer thin films, polymer materials with molecular additives and also polymer nanocomposites is that we must first theoretically understand and measure ΔH and ΔS of the neat bulk polymer reference system to understand the melt dynamics of the perturbed system at even elevated temperatures where glassy fluid dynamics is not a complicating factor.

In general, the activation parameters at high temperature should depend on film thickness since all these properties depend on the film thermodynamic properties.

T_0 [from equation (3.12)] gain insight into this fundamental problem for polymer fluid thin films, we consider what has been learned over time from the study of unentangled alkane fluids where large body of experimental and computational data exists.

First, we must understand how the polymeric nature of the fluid influences the activation parameters and then we consider the effect of confinement. Frankly, no fundamental predictive theory of the activation energy parameters of transition state theory for condensed disordered materials exists and our arguments must draw upon intuition, facts and phenomenology. Transition state theory retains its value as a general theoretical framework for organizing computational and experimental data under these circumstances.

It has been known for over 50 years that the activation energy for diffusion and viscosity of low molecular mass alkanes at high temperatures exhibits a strong dependence on chain molecular mass. This is a phenomenon exhibited by virtually all polymers. The typical range of activation energies typically involves roughly a factor of three increase in the activation energy ΔH as one increases the mass of the polymer from a monomer to an oligomeric polymer [104, 105] so the effect is rather large even in comparison with changes in the effective activation energy in glass-forming liquids where only a factor of 3 to 4 or so change in activation is required to understand the observed astronomical changes in relaxation times and diffusion in glass-forming liquids [106]. This significant variation of the activation energy with chain length is also generally observed in the beta relaxation time of polymeric materials [107], and the activation energy of polymer relaxation should similarly have such a strong mass dependence, a phenomenon of great significance for thin film measurements.

There is also much less discussed variation in the magnitude in the entropy of activation ΔS in polymer liquids such as alkanes. The pioneering study of ΔS by

Bondi [94] describes the frustrations of early theoretical efforts to estimate ΔS theoretically for complex fluids and he then notes that at least you can measure this quantity, assuming the applicability of transition state theory. These observations point to how we might model the variation of ΔS in our thin films, by extension. Recent simulation studies by Truskett and coworkers [108] and Charusita and coworkers [109] have also provided insights into the molecular variation of ΔS in polymer fluids and they have explored the relation between and the excess entropy of the fluid. DiMarzio and Yang have further argued for a connection between activation entropy ΔS and the configurational entropy of polymeric fluids, but no firm quantitative and general relation has been established [110].

According to Eyrings arguments [91], and long-standing physical observations on simple fluids, the high temperature enthalpy of activation is governed by the potential energy change associated with removal of one molecule from the environment of a test molecule and thus this quantity is proportional to the heat of vaporization or the cohesive interaction energy. The argument is simple, but this relation has established for hundreds of fluids and has recently been explored computationally by Egami and coworkers for metallic fluids [103]. The situation is evidently more complicated for polymer fluid where the cohesive interaction depends on the chain topology. For a melt of linear unentangled polymer chains, it is reasonable to assume they have random walk configurations because of the screening of excluded volume interactions in the condensed state. The polymer cohesive interaction should then scale as the number of polymer chain contacts which for a random walk chain scales as $\mathrm{c}n - \mathrm{d}n^{1/2}$ where c and d are constants; self-avoiding walks exhibit a similar scaling where the non-analytic correction to scaling exponent is somewhat modified [111]. If we take the activation energy for activation at elevated temperatures to scale with this basic measure of chain cohesive interaction then we can expect the activation enthalpy of polymer fluids

to scale as

$$\Delta H(\text{bulk unentangled polymer melt}) \simeq cn - dn^{1/2}. \tag{9.2}$$

Many authors have observed an approximately linear change in the activation energy of alkanes with chain length for both the viscosity η and diffusion coefficient D of low molecular mass alkanes [112, 113], and experiments over a large chain length range have shown that ΔH exhibits a progressively slower variation as n becomes as large as 20 to 30 carbon atoms [104], in qualitative accord with equation (9.2). The same qualitative trend in ΔH is exhibited in molecular dynamics simulations of η and D for alkanes [114]. Equation (9.2) points to an increase in the activation energy in polymers with an increase in the number of chain contact interactions, a phenomenon that makes perfect qualitative sense within a transition state framework. Correspondingly, it is natural to expect ΔS (bulk unentangled polymer melt) to be proportional to the entropy of a polymer chain under space filling conditions. For space-filling Hamilton walks, the chain entropy scales similarly to ΔH in equation (9.2), except the non-analytic correction to scaling exponent is then $(d-1)/d$ where d is the spatial dimension [115].

Bondi's analysis [94] of ΔS for low molecular mass linear alkanes (up to 40 carbon atoms in molecule) at elevated temperatures, where an Arrhenius temperatures is applicable, shows an n variation for ΔS mirrors that suggested for ΔH above (see figure 6 of Bondi [94]) so the predicted strong n variation of ΔS for polymer melts is apparently observed. Recently, the strong variation of ΔS alkanes has been noted as being important for understanding the effect of polymer structure on catalytic reactions (cracking of alkanes and other reactions on zeolitic catalysts) [84, 116, 117] so this phenomenon is expected to have rather broad practical significance beyond the finite size effects on glassy dynamics considered in the present paper.

We are then proposing that the enthalpic and entropic energetic parameters governing configurational free energy of the polymers in the melt govern, at least in their general scaling form with chain mass, the activation enthalpy and entropies of activation of polymer fluids. This is crucial for the analysis of this thesis since this model points to how confinement might alter the activation free energy parameters since it is generally understood how confinement alters the configurational properties of polymers, modeled as random walks.

9.2 Influence of Confinement on Activation Energy Parameters

We consider $\Delta S(h)$ to be generally dependent on film thickness because of the inherently relative high activation energies ΔH of transport in polymer materials is normally found in condensed materials to give a proportionate contribution to ΔS [97, 118]. This important relation between the enthalpy and entropy activation energies directly mirrors Troutons rule [119, 120], a proportionate relation between the heat of vaporization and the entropy of vaporization of gases and the Barclay-Butler phenomenological relation linking enthalpies and entropies of solvation in many mixtures [121–124]. From the general link between activation enthalpy ΔH and the heat of vaporization so the activation energy can naturally be expected to be linked in the same fashion (See Ref. [94]). Indeed many studies have established and attempted to rationalize the specific functional relation supported by observations on impressively diverse materials [95–97],

$$\Delta S = \Delta S_{\mathrm{o}} + \Delta H / k_{\mathrm{B}} T_{\mathrm{comp}} \tag{9.3}$$

and this linear relation has long been established in Arrhenius activation parameters of bulk polymer fluids [125, 126]. In diluted glass-forming materials,

the entropy-enthalpy compensation temperature $T_{\rm comp}$ in this relation has been suggested [127] to be generally near the glass transition temperature and measurements on the glass-forming liquid trehalose and polycarbonate with additives indicated that this temperature was comparable to the VFT temperature T_0 [128, 129]. We anticipate a similar trend in the dynamics of thin polymer film generally, but this remains to be established through comparison to experiment and measurement where such an effect would be rather conspicuous experimentally. We also note that ΔS can have a purely entropic contribution in the case of athermal systems such as hard spheres where the energetic barriers are predominantly entropic in nature and the term $\Delta S_{\rm o}$ in equattion (9.3) dominates the activation free energy when enthalpic interaction effects are weak so that ΔH can be neglected [61]. We test these predicted relations in our simulations of supported polymer films and find them to be remarkable supported by our simulation data.

The development of long range collective motion in condensed materials necessitates a further extension of our model expression for τ for thin films. Within the simple Adam-Gibbs model for bulk materials, this effect is accounted for by simply multiplying the activation free energy ΔG by the extent of cooperative motion z^*, which we have formerly established. Specifically we found z^* can be identified quantitatively with the average length of string-like collective motion, L [55, 60]. In thin films, it is not clear how collective motion alters the change in ΔS associated with confinement, but it seems reasonable to adopt the tentative relation,

$$\tau(T) = \tau_\infty(\text{bulk}) \exp\left[-(aR_g/h)^\alpha \right] \exp\left[\frac{L(T)}{T}(\Delta H - T\Delta S) \right] \qquad (9.4)$$

which is the functional relation that we explore in our simulation data. According to this relation we also find the chain conformational entropy be related to the system size, described in Chapter 6.

Bibliography

[1] Richard P Feynman. There's plenty of room at the bottom. *Engineering and Science*, 23(5):22–36, 1960.

[2] Charles P. Poole, Frank J. Jones, and Frank J. Owens. *Introduction to Nanotechnology*. John Wiley & Sons, Inc., New York, 2003.

[3] G. Silva. Introduction to nanotechnology and its applications to medicine. *Surgical Neurology*, 61(3):216–220, March 2004.

[4] Marie-Christine Daniel and Didier Astruc. Gold nanoparticles: assembly, supramolecular chemistry, quantum-size-related properties, and applications toward biology, catalysis, and nanotechnology. *Chem. Rev.*, 104(1):293–346, 2004.

[5] D.R. Paul and L.M. Robeson. Polymer nanotechnology: Nanocomposites. *Polymer*, 49(15):3187 – 3204, 2008.

[6] Toshikatsu Tanaka, GC Montanari, and R Mulhaupt. Polymer nanocomposites as dielectrics and electrical insulation-perspectives for processing technologies, material characterization and future applications. *Dielectrics and Electrical Insulation, IEEE Transactions on*, 11(5):763–784, 2004.

[7] WA MacDonald, MK Looney, D MacKerron, R Eveson, R Adam,

K Hashimoto, and K Rakos. Latest advances in substrates for flexible electronics. *J. Soc. Information Display*, 15(12):1075–1083, 2007.

[8] P. G. Debenedetti and F. H. Stillinger. Supercooled liquids and the glass transition. *Nature*, 410(6825):259–267, MAR 8 2001.

[9] C. A. Angell. Formation of glasses from liquids and biopolymers. *Science*, 267:1924, 1995.

[10] Ernst-Joachim Donth. *The glass transition: relaxation dynamics in liquids and disordered materials*, volume 48. Springer, Berlin, 2001.

[11] W Götze. The essentials of the mode-coupling theory for glassy dynamics. *Condens. Matter Phys*, 4:873–904, 1998.

[12] S Guilbert, N Gontard, and B Cuq. Technology and applications of edible protective films. *Packaging Technology and Science*, 8(6):339–346, 1995.

[13] D. Bratton, D. Yang, J. Y. Dai, and C. K. Ober. Recent progress in high resolution lithography. *Polym. Adv. Tech.*, 17(2):94–103, FEB 2006.

[14] D. W. Hutmacher. Scaffold design and fabrication technologies for engineering tissues - state of the art and future perspectives. *J. Biomat. Sci. Polym. Ed.*, 12(1):107–124, 2001.

[15] Joseph L. Keddie, Richard A. L. Jones, and Rachel A. Cory. Size-dependent depression of the glass transition temperature in polymer films. *Europhys. Lett.*, 27:59–64, 1994.

[16] J. A. Forrest, K. Dalnoki-Veress, and J. R. Dutcher. Interface and chain confinement effects on the glass transition temperature of thin polymer films. *Phys. Rev. E*, 56(5, Part B):5705–5716, NOV 1997.

[17] Koji Fukao and Yoshihisa Miyamoto. Slow dynamics near glass transitions in thin polymer films. *Phys. Rev. E*, 64:011803, Jun 2001.

[18] D. S. Fryer, R. D. Peters, E. J. Kim, J. E. Tomaszewski, J. J. de Pablo, P. F. Nealey, C. C. White, and W. L. Wu. Dependence of the glass transition temperature of polymer films on interfacial energy and thickness. *Macromolecules*, 34(16):5627–5634, JUL 31 2001.

[19] C. J. Ellison and J. M. Torkelson. The distribution of glass-transition temperatures in nanoscopically confined glass formers. *Nature Materials*, 2(10):695–700, OCT 2003.

[20] M. Alcoutlabi and G. B. McKenna. Effects of confinement on material behaviour at the nanometre size scale. *J. Phys Condens. Matter*, 17(15):R461–R524, APR 20 2005.

[21] A. Bansal, H. C. Yang, C. Z. Li, K. W. Cho, B. C. Benicewicz, S. K. Kumar, and L. S. Schadler. Quantitative equivalence between polymer nanocomposites and thin polymer films. *Nature Materials*, 4(9):693–698, SEP 2005.

[22] R. D. Priestley, C. J. Ellison, L. J. Broadbelt, and J. M. Torkelson. Structural relaxation of polymer glasses at surfaces, interfaces and in between. *Science*, 309(5733):456–459, JUL 15 2005.

[23] S. Kim, S. A. Hewlett, C. B. Roth, and J. M. Torkelson. Confinement effects on glass transition temperature, transition breadth, and expansivity: Comparison of ellipsometry and fluorescence measurements on polystyrene films. *Eur. Phys. J. E*, 30(1):83–92, SEP 2009.

[24] J. A. Torres, P. F. Nealey, and J. J. de Pablo. Molecular simulation of ultra-

thin polymeric films near the glass transition. *Phys. Rev. Lett.*, 85(15):3221–3224, OCT 9 2000.

[25] Grant D. Smith, Dmitry Bedrov, and Oleg Borodin. Structural relaxation and dynamic heterogeneity in a polymer melt at attractive surfaces. *Phys. Rev. Lett.*, 90:226103, Jun 2003.

[26] J. Baschnagel and F. Varnick. Computer simulation of supercooled polymers melt in the bulk and confined geometry. *Condensed Matter*, 17(R851):852–945, 2005.

[27] Robert A. Riggleman, Kenji Yoshimoto, Jack F. Douglas, and Juan J. de Pablo. Influence of confinement on the fragility of antiplasticized and pure polymer films. *Phys. Rev. Lett.*, 97(4):045502, JUL 28 2006.

[28] S. Peter, H. Meyer, and J. Baschnagel. Molecular dynamics simulations of concentrated polymer solutions in thin film geometry. i. equilibrium properties near the glass transition. *J. Chem. Phys.*, 131(1):014902, JUL 7 2009.

[29] Jean-Louis Barrat, Jorg Baschnagel, and Alexey Lyulin. Molecular dynamics simulations of glassy polymers. *Soft Matter*, 6:3430–3446, 2010.

[30] Christopher M. Stafford, Bryan D. Vogt, Christopher Harrison, Duangrut Julthongpiput, and Rui Huang. Elastic moduli of ultrathin amorphous polymer films. *Macromolecules*, 39(15):5095–5099, jun 2006.

[31] Paul A. O'Connell, Stephen A. Hutcheson, and Gregory B. McKenna. Creep behavior of ultra-thin polymer films. *J. Polym. Sci. B*, 46(18):1952–1965, 2008.

[32] Kurt Binder, Juergen Horbach, Richard Vink, and Andres De Virgiliis. Con-

finement effects on phase behavior of soft matter systems. *Soft Matter*, 4(8):1555–1568, 2008.

[33] J. A. Forrest, K. Dalnoki-Veress, J. R. Stevens, and J. R. Dutcher. Effect of free surfaces on the glass transition temperature of thin polymer films. *Phys. Rev. Lett.*, 77(10):2002–2005, SEP 2 1996.

[34] Keewook Paeng, Ranko Richert, and M. D. Ediger. Molecular mobility in supported thin films of polystyrene, poly(methyl methacrylate), and poly(2-vinyl pyridine) probed by dye reorientation. *Soft Matter*, 8:819–826, 2012.

[35] C. J. Ellison, S. D. Kim, D. B. Hall, and J. M. Torkelson. Confinement and processing effects on glass transition temperature and physical aging in ultrathin polymer films: Novel fluorescence measurements. *Eur. Phys. J. E*, 8(2):155–166, MAY 2002.

[36] A. Schönhals, H. Goering, Ch Schick, B. Frick, and R. Zorn. Glassy dynamics of polymers confined to nanoporous glasses revealed by relaxational and scattering experiments. *Eur. Phys. J. E*, 12(1):173–178, September 2003.

[37] S. Kawana and R. A. L. Jones. Character of the glass transition in thin supported polymer films. *Phys. Rev. E*, 63(2, Part 1):021501, FEB 2001.

[38] Simone Peter, Hendrik Meyer, and Jorg Baschnagel. Thickness-dependent reduction of the glass-transition temperature in thin polymer films with a free surface. *J. Polym. Sci. B*, 44(20):2951–2967, OCT 15 2006.

[39] Paul Z Hanakata, Jack F Douglas, and Francis W Starr. Local variation of fragility and glass transition temperature of ultra-thin supported polymer films. *J. Chem. Phys.*, 137:244901, 2012.

[40] G. B. DeMaggio, W. E. Frieze, D. W. Gidley, Ming Zhu, H. A. Hristov,

and A. F. Yee. Interface and surface effects on the glass transition in thin polystyrene films. *Phys. Rev. Lett.*, 78:1524–1527, Feb 1997.

[41] D. Long and F. Lequeux. Heterogeneous dynamics at the glass transition in van der waals liquids, in the bulk and in thin films. *Eur. Phys. J. E*, 4(3):371–387, March 2001.

[42] PG de Gennes. Glass transitions in thin polymer films. *Eur. Phys. J. E*, 2(3):201–203, JUL 2000.

[43] Michael Erber, Martin Tress, Emmanuel U. Mapesa, Anatoli Serghei, Klaus-Jochen Eichhorn, Brigitte Voit, and Friedrich Kremer. Glassy dynamics and glass transition in thin polymer layers of pmma deposited on different substrates. *Macromolecules*, 43(18):7729–7733, 2010.

[44] Ranjeet S. Tate, David S. Fryer, Silvia Pasqualini, Martha F. Montague, Juan J. de Pablo, and Paul F. Nealey. Extraordinary elevation of the glass transition temperature of thin polymer films grafted to silicon oxide substrates. *J. Chem. Phys.*, 115(21):9982–9990, 2001.

[45] Qianqian Tong and S. J. Sibener. Visualization of individual defect mobility and annihilation within cylinder-forming diblock copolymer thin films on nanopatterned substrates. *Macromolecules*, 46(21):8538–8544, 2013.

[46] Connie B. Roth, Katie L. McNerny, Wolter F. Jager, and John M. Torkelson. Eliminating the enhanced mobility at the free surface of polystyrene, fluorescence studies of the glass transition temperature in thin bilayer films of immiscible polymers. *Macromolecules*, 40(7):2568–2574, 2007.

[47] G. Adam and J. H. Gibbs. On temperature dependence of cooperative

relaxation properties in glass-forming liquids. *J. Chem. Phys.*, 43(1):139–&, 1965.

[48] T. R. Kirkpatrick, D. Thirumalai, and P. G. Wolynes. Scaling concepts for the dynamics of viscous liquids near an ideal glassy state. *Phys. Rev. A*, 40:1045–1054, Jul 1989.

[49] C. Donati, J. F. Douglas, W. Kob, S. J. Plimpton, P. H. Poole, and S. C. Glotzer. Stringlike cooperative motion in a supercooled liquid. *Phys. Rev. Lett.*, 80(11):2338–2341, MAR 16 1998.

[50] M. Aichele, Y. Gebremichael, F. W. Starr, J. Baschnagel, and S. C. Glotzer. Polymer-specific effects of bulk relaxation and stringlike correlated motion in the dynamics of a supercooled polymer melt. *J. Chem. Phys.*, 119(10):5290–5304, SEP 8 2003.

[51] Y Gebremichael, M Vogel, and SC Glotzer. Particle dynamics and the development of string-like motion in a simulated monoatomic supercooled liquid. *J. Chem. Phys.*, 120(9):4415–4427, MAR 1 2004.

[52] M Vogel, B Doliwa, A Heuer, and SC Glotzer. Particle rearrangements during transitions between local minima of the potential energy landscape of a binary lennard-jones liquid. *J. Chem. Phys.*, 120(9):4404–4414, MAR 1 2004.

[53] TB Schroder, S Sastry, JC Dyre, and SC Glotzer. Crossover to potential energy landscape dominated dynamics in a model glass-forming liquid. *J. Chem. Phys.*, 112(22):9834–9840, JUN 8 2000.

[54] N Giovambattista, F W Starr, F Sciortino, S V Buldyrev, and H E Stanley.

Transitions between inherent structures in water. *Phys. Rev. E*, 65(4, Part 1), APR 2002.

[55] Francis W Starr, Jack F Douglas, and Srikanth Sastry. The relationship of dynamical heterogeneity to the adam-gibbs and random first-order transition theories of glass formation. *J. Chem. Phys.*, 138:12A541, 2013.

[56] Zhongyu Zheng, Feng Wang, and Yilong Han. Glass transitions in quasi-two-dimensional suspensions of colloidal ellipsoids. *Phys. Rev. Lett.*, 107:065702, Aug 2011.

[57] Andrew H. Marcus, Jeremy Schofield, and Stuart A. Rice. Experimental observations of non-gaussian behavior and stringlike cooperative dynamics in concentrated quasi-two-dimensional colloidal liquids. *Phys. Rev. E*, 60:5725–5736, Nov 1999.

[58] Zexin Zhang, Peter J. Yunker, Piotr Habdas, and A. G. Yodh. Cooperative rearrangement regions and dynamical heterogeneities in colloidal glasses with attractive versus repulsive interactions. *Phys. Rev. Lett.*, 107:208303, Nov 2011.

[59] Eric R. Weeks, J. C. Crocker, Andrew C. Levitt, Andrew Schofield, and D. A. Weitz. Three-dimensional direct imaging of structural relaxation near the colloidal glass transition. *Science*, 287(5453):627–631, 2000.

[60] F. W. Starr and J. F. Douglas. Modifying fragility and collective motion in polymer melts with nanoparticles. *Phys. Rev. Lett.*, 106:115702, 2011.

[61] Beatriz A. Pazmino Betancourt, Jack F. Douglas, and Francis W. Starr. Fragility and cooperative motion in a glass-forming polymer-nanoparticle composite. *Soft Matter*, 9:241–254, 2013.

[62] Jacob D. Stevenson and Peter G. Wolynes. On the surface of glasses. *J. Chem. Phys.*, 129(23):–, 2008.

[63] Ryan J. Lang and David S. Simmons. Interfacial dynamic length scales in the glass transition of a model freestanding polymer film and their connection to cooperative motion. *Macromolecules*, 46(24):9818–9825, 2013.

[64] Dmytro Hudzinskyy, Alexey V. Lyulin, Arlette R. C. Baljon, Nikolay K. Balabaev, and Matthias A. J. Michels. Effects of strong confinement on the glass-transition temperature in simulated atactic polystyrene films. *Macromolecules*, 44(7):2299–2310, 2011.

[65] Chrysostomos Batistakis, Alexey V. Lyulin, and M. A. J. Michels. Slowing down versus acceleration in the dynamics of confined polymer films. *Macromolecules*, 45(17):7282–7292, 2012.

[66] M. P. Allen and D. J. Tildesley. *Computer Simulation of Liquids*. Oxford science publications. Oxford, June 1989.

[67] G. S. Grest and K. Kremer. Molecular-dynamics simulation for polymers in the presence of a heat bath. *Phys. Rev. A*, 33:3628, 1986.

[68] Mark E. Mackura and David S. Simmons. Enhancing heterogenous crystallization resistance in a bead-spring polymer model by modifying bond length. *J. Polym. Sci. B*, 52(2):134–140, 2014.

[69] MBBJM Tuckerman, Bruce J Berne, and Glenn J Martyna. Reversible multiple time scale molecular dynamics. *J. Chem. Phys.*, 97(3):1990–2001, 1992.

[70] D. Sidebottom, R. Bergman, L. Börjesson, and L. M. Torell. Two-step

relaxation decay in a strong glass former. *Phys. Rev. Lett.*, 71:2260–2263, Oct 1993.

[71] S. Peter, S. Napolitano, H. Meyer, M. Wubbenhorst, and J. Baschnagel. Modeling dielectric relaxation in polymer glass simulations: Dynamics in the bulk and in supported polymer films. *Macromolecules*, 41(20):7729–7743, OCT 28 2008.

[72] Henry Eyring. Viscosity, plasticity, and diffusion as examples of absolute reaction rates. *J. Chem. Phys.*, 4(4):283–291, 1936.

[73] F. W. Starr, J. F. Douglas, and S. C. Glotzer. Origin of particle clustering in a simulated polymer nanocomposite and its impact on rheology. *J. Chem. Phys.*, 119(3):1777–1788, JUL 15 2003.

[74] Qian Qin and Gregory B. McKenna. Correlation between dynamic fragility and glass transition temperature for different classes of glass forming liquids. *J. Non-Cryst. Solids*, 352(28-29):2977–2985, AUG 15 2006.

[75] C. Donati, S. C. Glotzer, P. H. Poole, W. Kob, and S. J. Plimpton. Spatial correlations of mobility and immobility in a glass-forming lennard-jones liquid. *Phys. Rev. E*, 60(3):3107–3119, SEP 1999.

[76] Yeshitila Gebremichael, Michael Vogel, Magnus N. J. Bergroth, Francis W. Starr, and Sharon C. Glotzer. Spatially heterogeneous dynamics and the adam-gibbs relation in the dzugutov liquid. *J. Phys. Chem. B*, 109(31):15068–15079, 2005. PMID: 16852907.

[77] P. Scheidler, W. Kob, and K. Binder. Cooperative motion and growing length scales in supercooled confined liquids. *Europhys. Lett.*, 59(5):701, 2002.

[78] A. Virgiliis, A. Milchev, V.G. Rostiashvili, and T.A. Vilgis. Structure and dynamics of a polymer melt at an attractive surface. *Eur. Phys. J. E*, 35(9):1–11, 2012.

[79] K Binder, J Baschnagel, and W Paul. Glass transition of polymer melts: test of theoretical concepts by computer simulation. *Prog. Polym. Sci.*, 28(1):115–172, JAN 2003.

[80] Jeetain Mittal, Jeffrey R. Errington, and Thomas M. Truskett. Thermodynamics predicts how confinement modifies the dynamics of the equilibrium hard-sphere fluid. *Phys. Rev. Lett.*, 96:177804, May 2006.

[81] F. W. Starr, P. Z. Hanakata, B. A. Pazmino Betancourt, S. Sastry, and J. F. Douglas. *Fragility and Cooperative Motion in Polymer Glass Formation.* Fragility of glass forming liquids, 2014.

[82] Claudio Donati, Jack F. Douglas, Walter Kob, Steven J. Plimpton, Peter H. Poole, and Sharon C. Glotzer. Stringlike cooperative motion in a supercooled liquid. *Phys. Rev. Lett.*, 80:2338–2341, Mar 1998.

[83] M Aichele, Y Gebremichael, Francis Starr, J Baschnagel, and SC Glotzer. Stringlike correlated motion in the dynamics of supercooled polymer melts. *J. Chem. Phys.*, 119:5290–5304, 2003.

[84] C. M. Guttman, E. A. Di Marzio, and J. F. Douglas. Influence of polymer architecture and polymersurface interaction on the elution chromatography of macromolecules through a microporous media. *Macromolecules*, 29(17):5723–5733, 1996.

[85] David C. Lin, Jack F. Douglas, and Ferenc Horkay. Development of minimal

models of the elastic properties of flexible and stiff polymer networks with permanent and thermoreversible cross-links. *Soft Matter*, 6:3548–3561, 2010.

[86] J. Dayantis and J. Sturm. Monte-carlo calculations on statistical chains enclosed inside a sphere. *Polymer*, 26(11):1631 – 1637, 1985.

[87] C Domb. Critical temperature of finite systems in d dimensions. *J. Phys. A*, 6(9):1296, 1973.

[88] Hao Zhang and Jack F. Douglas. Glassy interfacial dynamics of ni nanoparticles: part i colored noise, dynamic heterogeneity and collective atomic motion. *Soft Matter*, 9:1254–1265, 2013.

[89] Keiji Watanabe, Takeshi Kawasaki, and Hajime Tanaka. Structural origin of enhanced slow dynamics near a wall in glass-forming systems. *Nat Mater*, 10(7):512–520, July 2011.

[90] Raymond H. Ewell. The reaction rate theory of viscosity and some of its applications. *J. Appl. Phys.*, 9(4):252–269, 1938.

[91] S. Glasstone, Keith J. Laidler, and Henry Eyring. *Theory of Rate Processes*. McGraw Hill, first edition edition, 1941.

[92] Walter Kauzmann and Henry Eyring. The viscous flow of large molecules. *J. Am. Chem. Soc.*, 62(11):3113–3125, 1940.

[93] Henry Eyring, Taikyue Ree, and Nishio Hirai. The viscosity of high polymersthe random walk of a group of connected segments. *Proc. Natl. Acad. Sci. USA*, 44(12):1213–1217, 1958.

[94] A. Bondi. Notes on the rate process theory of flow. *J. Chem. Phys.*, 14(10):591–607, 1946.

[95] A Yelon, B Movaghar, and R S Crandall. Multi-excitation entropy: its role in thermodynamics and kinetics. *Rep. Prog. Phys.*, 69(4):1145, 2006.

[96] Arthur Yelon, Edward Sacher, and Wolfgang Linert. Multi-excitation entropy, entropyenthalpy relations, and their impact on catalysis. *Catalysis Letters*, 141(7):954–957, 2011.

[97] A. Yelon and B. Movaghar. Microscopic explanation of the compensation (meyer-neldel) rule. *Phys. Rev. Lett.*, 65:618–620, Jul 1990.

[98] E. W. Madge. The viscosities of liquids and their vapor pressures. *J. Appl. Phys.*, 5(2):39–41, 1934.

[99] F. Eirich and R. Simha. A contribution to the theory of viscous flow reactions for chainlike molecular substances. *J. Chem. Phys.*, 7(2):116–121, 1939.

[100] Lei Qun-Fang, Hou Yu-Chun, and Lin Rui-Sen. Correlation of viscosities of pure liquids in a wide temperature range. *Fluid Phase Equilibria*, 140(12):221 – 231, 1997.

[101] R.J. Speedy, F.X. Prielmeier, T. Vardag, E.W. Lang, and H.-D. Ldemann. Diffusion in simple fluids. *Mol. Phys.*, 66(3):577–590, 1989.

[102] H. G. E. Hentschel, S. Karmakar, I. Procaccia, and J. Zylberg. Relaxation Mechanisms in Glassy Dynamics: the Arrhenius and Fragile Regimes. *ArXiv e-prints*, February 2012.

[103] T. Iwashita, D. M. Nicholson, and T. Egami. Elementary excitations and crossover phenomenon in liquids. *Phys. Rev. Lett.*, 110:205504, May 2013.

[104] David Tabor. Micromolecular processes in the viscous flow of hydrocarbons. *Philos. Mag. A*, 57(2):217–224, 1988.

[105] V. Arrighi, J. Tanchawanich, and Mark T. F. Telling. Molar mass dependence of polyethylene chain dynamics. a quasi-elastic neutron scattering investigation. *Macromolecules*, 46(1):216–225, 2013.

[106] Jacek Dudowicz, Karl F. Freed, and Jack F. Douglas. Generalized entropy theory of polymer glass formation. *Adv. Chem. Phys.*, 137:125–222, 2008.

[107] V.A Bershtein and V.M Yegorov. General mechanism of the transition in polymers. *Polym. Sci. U.S.S.R.*, 27(11):2743 – 2757, 1985.

[108] Ravi Chopra, Thomas M. Truskett, and Jeffrey R. Errington. On the use of excess entropy scaling to describe single-molecule and collective dynamic properties of hydrocarbon isomer fluids. *J. Phys. Chem. B*, 114(49):16487–16493, 2010.

[109] Teena Goel, Chandra Nath Patra, Tulsi Mukherjee, and Charusita Chakravarty. Excess entropy scaling of transport properties of lennard-jones chains. *J. Chem. Phys.*, 129(16):–, 2008.

[110] Di Marzio EA and AJM Yang. Configurational entropy approach to the kinetics of glasses. *J. Res. Natl. Inst. Stand. Technol.*, 102:135, 1997.

[111] Jack F. Douglas and Takao Ishinabe. Self-avoiding-walk contacts and random-walk self-intersections in variable dimensionality. *Phys. Rev. E*, 51:1791–1817, Mar 1995.

[112] Robert Zwanzig and Alan K. Harrison. Modifications of the stokeseinstein formula. *J. Chem. Phys.*, 83(11):5861–5862, 1985.

[113] W. R. Moore. Entropy of activation of viscous flow in dilute solutions of high polymers. *Nature*, 204(4980):184184, 1965.

[114] Song-Hi Lee. Molecular dynamics simulation studies of viscosity and dif-

fusion of n-alkane oligomers at high temperatures. *Bull. Krn. Chem. Soc.*, 32:3909–3913, 2011.

[115] Jack Douglas, Charles M. Guttman, Alex Mah, and Takao Ishinabe. Spectrum of self-avoiding walk exponents. *Phys. Rev. E*, 55:738–749, Jan 1997.

[116] Aditya Bhan, Rajamani Gounder, Josef Macht, and Enrique Iglesia. Entropy considerations in monomolecular cracking of alkanes on acidic zeolites. *J. Catalysis*, 253(1):221 – 224, 2008.

[117] Rajamani Gounder and Enrique Iglesia. The roles of entropy and enthalpy in stabilizing ion-pairs at transition states in zeolite acid catalysis. *Acc. Chem. Res.*, 45(2):229–238, 2012.

[118] G. Boisvert, N. Mousseau, and L. J. Lewis. Comment on "role of lattice vibrations in adatom diffusion". *Phys. Rev. Lett.*, 80:203–203, Jan 1998.

[119] Rafael M Digilov and M Reiner. Trouton's rule for the law of corresponding states. *Eur. J. Phys.*, 25(1):15, 2004.

[120] Leonard K. Nash. Trouton and t-h-e rule. *J. Chem. Ed.*, 61(11):981, 1984.

[121] I. M. Barclay and J. A. V. Butler. The entropy of solution. *Trans. Faraday Soc.*, 34:1445–1454, 1938.

[122] R. P. Bell. Relations between the energy and entropy of solution and their significance. *Trans. Faraday Soc.*, 33:496–501, 1937.

[123] M. G. Evans and M. Polanyi. Further considerations on the thermodynamics of chemical equilibria and reaction rates. *Trans. Faraday Soc.*, 32:1333–1360, 1936.

[124] Henry S. Frank. Free volume and entropy in condensed systems ii. entropy

of vaporization in liquids and the pictorial theory of the liquid state. *J. Chem. Phys.*, 13(11):493–507, 1945.

[125] R. M. Barrer. Viscosity of pure liquids. i. non-polymerised fluids. *Trans. Faraday Soc.*, 39:48–59, 1943.

[126] Chas. E. Waring and Paul Becher. Structure in liquids and the relation between the parameters of the arrhenius equation for reactions in the condensed phase. *J. Chem. Phys.*, 15(7):488–496, 1947.

[127] J C Dyre. A phenomenological model for the meyer-neldel rule. *J. Phys. C*, 19(28):5655, 1986.

[128] A. Anopchenko, T. Psurek, D. VanderHart, J. F. Douglas, and J. Obrzut. Dielectric study of the antiplasticization of trehalose by glycerol. *Phys. Rev. E*, 74:031501, Sep 2006.

[129] Tatiana Psurek, Christopher L. Soles, Kirt A. Page, Marcus T. Cicerone, and Jack F. Douglas. Quantifying changes in the high-frequency dynamics of mixtures by dielectric spectroscopy. *J. Phys. Chem. B*, 112(50):15980–15990, 2008.